



Synthesis and antitumor activity of novel gibberellin derivatives with tetracyclic diterpenoid skeletons

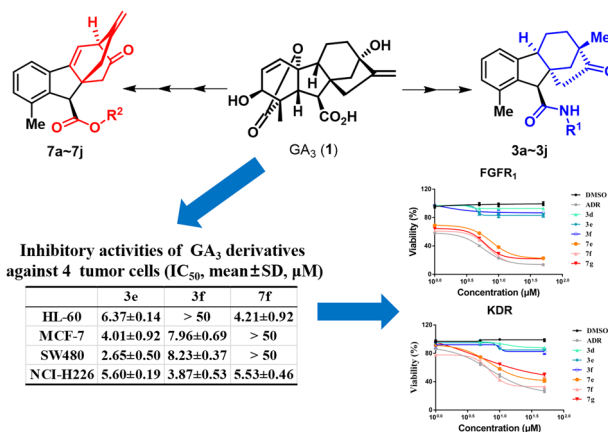
Shi-ying Zhu¹ · Fa-zeng Luo¹ · Ping-Hua Sun¹

Received: 15 February 2020 / Accepted: 27 April 2020
© Springer Science+Business Media, LLC, part of Springer Nature 2020

Abstract

Gibberellic acid (GA₃) is a tetracyclic diterpene compound which displays interesting bioactivities. Recently, its potential use for preparing antitumor drug leads has been highlighted, and various modification methods of GA₃ have been reported. Aiming at investigating GA₃ derivatives with potential antitumor activities, ring distortion of GA₃ under different conditions was carried out, and this was followed with amidation or substitution, yielding four series of derivatives. The chemical structure of these compounds were analyzed by ¹H-NMR, ¹³C-NMR, HRMS, FTIR and polarimetry, and SXRD was employed to further confirm the spatial configurations of derivatives **3c** and **7d**. The antitumor activities of three series of derivatives were evaluated by using MTT assay and ELISA. Results shows that, among amide derivatives, compounds with a saturated linear amide showed better activity than those with an aromatic amide. Among ester derivatives, compounds with a *meta*-substituted benzyl group showed better activities than those with a *para*-substituted benzyl group. The antitumor activity of ester derivatives might possibly be linked with the inhibition of FGFR₁ activation and KDR activation. Overall, this study discussed how the antitumor activity of GA₃ was formed, thereby assisting the future design of more effective active GA₃ derivatives.

Graphical Abstract



Keywords Gibberellic acid · Modification of GA₃ · Ring-distortion · Antitumor · MTT assay and ELISA

Supplementary information The online version of this article (<https://doi.org/10.1007/s00044-020-02551-2>) contains supplementary material, which is available to authorized users.

✉ Ping-Hua Sun
pinghuasunny@163.com

¹ Guangdong Engineering Research Center of Chinese Medicine & Disease Susceptibility, College of Pharmacy, Jinan University, Guangzhou 510632, China

Introduction

The creation of complex and diverse small molecules from natural products are important resource for new drug leads (Huigens et al. 2013). These structurally complex natural products have been a significant inspiration for the design and synthesis of bioactive compounds in the history of drug discovery (Wu et al. 2018; Mander 2003). The gibberellins (GAs) are a large class of tetracyclic diterpene compounds that are presented in a wide range of higher-order plants and fungi where they act as phytohormones to regulate various plant developmental processes (Mander 1992). The profound effects of GAs on plants make them a useful agricultural chemical in modern agriculture to increase crop yields (Grigor and Kucherov 1966). Certain GAs such as GA₃ (**1**) also acts as a versatile material in construction of structurally diverse compounds as well as bioactive agents (Wu et al. 2018; Mander 2003; Chen et al. 2009; Egbewande et al. 2018).

According to their biosynthetic pathway (Bon et al. 2018), the metabolic precursor of GAs are *ent*-kaurenes. The antitumor activities of many *ent*-kaurene type tetracyclic diterpenes have been reported (Fig. 1). For instance, amethystoidin A, which presents in leaves of *Rabdosia* (*Bl*) *Hassk* plants, shows antitumor and antibacterial effects (Liu et al. 2017); oridonin and ponidicin are effective components in *Rabdosia rubescens*, a traditional Chinese herb medicine used to treat esophagus cancer and gastric cancer (Egbewande et al. 2018; He et al. 2009; Sun et al. 1992).

Ent-kaurane diterpenoids exhibit considerable biological activities, including antitumor, antibacterial, anti-tuberculosis, and anti-inflammatory effects. For example, *Pharicin B*, a novel natural *ent*-kaurene diterpenoid, can induce clinically remission in most acute promyelocytic leukemia patients (Gu et al. 2010). Three new *ent*-kaurane diterpenes were isolated from the herbs of *Wedelia prostrata* and evaluated for their cytotoxic activity on HepG2 cells, with their IC₅₀ values ranging from 9.55 ± 0.45 to 53.92 ± 1.22 μM (Wu et al. 2017). Lin et al. reported the discovery of new *ent*-kaurane diterpenoids, and found some alkaline and amide derivatives which showed good selectivity on human cancer cell lines (Lin et al. 2015).

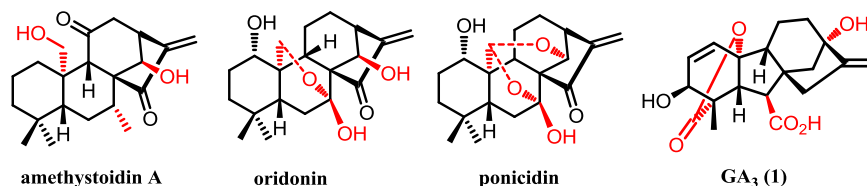
Inspired by the structural connection between GAs with *ent*-kaurenes, J. Chen et al. reported the first antitumor properties of a series of GA₃ derivatives bearing two α, β-unsaturated ketone units (Chen et al. 2009). Recently, Wu

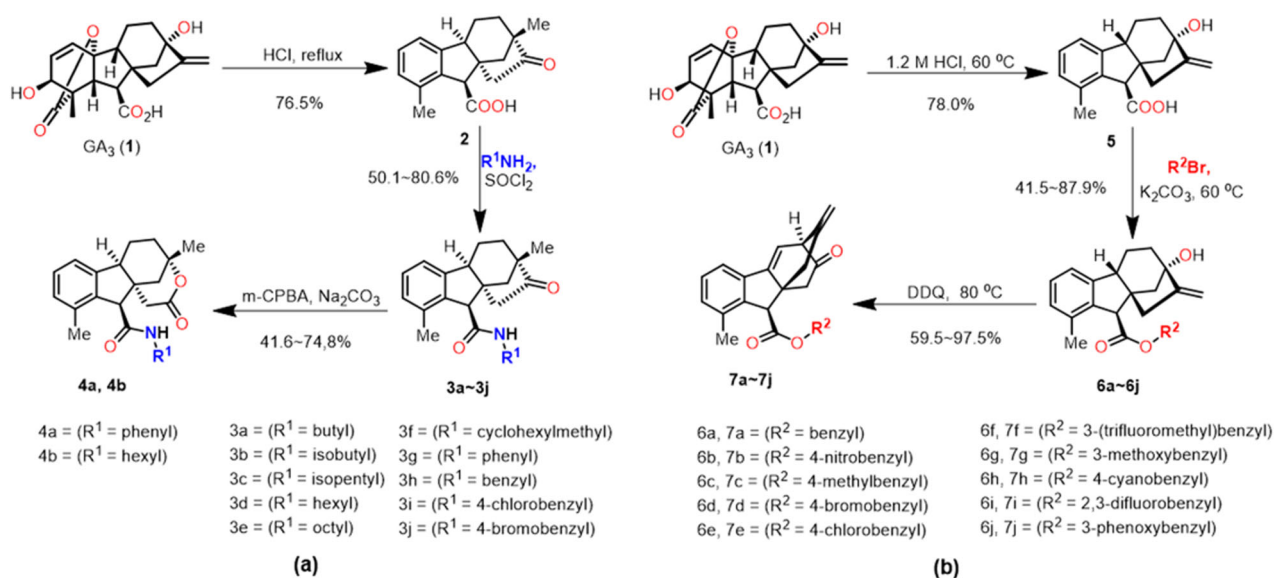
et al. designed and prepared a series of allogibberic acid derivatives that contain the 1,2,3-triazole pharmacophore, and found that three of these derivatives displayed broad anticancer activities, presumably via inducing S phase arrest in the cell cycle (Wu et al. 2018; Cross et al. 1958). Moreover, Egbewande et al. prepared a series of amide derivatives based on the scaffold GA₃, and their potencies in deregulation of lipid metabolism in human prostate cancer cell line (LNCaP) were evaluated, which revealed that certain amide derivatives greatly decreased the uptake free cholesterol and resulted in deregulation of intracellular cholesterol metabolism (Egbewande et al. 2018). Based on their findings, we came up with the opinion that GA₃ would readily be rearranged and isomerized under mild conditions due to its special arrangement of functional groups. Given the promising bioactivities of GA₃ derivatives and the available preparation method of diverse derivatives from GA₃ (Huigens et al. 2013), we aim to synthesize four types of GA₃ derivatives by means of ring-distortion, amination, esterification, and/or ring rearrangements. Twenty-two novel compounds were obtained, and their anti-proliferative activity as well as possible mechanism of action have been explored via MTT assay and enzyme linked immunosorbent assay (ELISA). A comparison of amide and ester derivatives will show us their selectivity on various human cancer cell lines.

Due to the arrangements of functional groups of GA₃, skeletal diversifications and isomerization are readily take place under mild conditions. For instance, using mineral acids, GA₃ can undergo aromatization to yield rearrangement products, such as gibberic acid (**2**) and allogibberic acid (**5**) (Cross et al. 1958; Mulholland 1958). In both conversions, the γ-lactone ring of GA₃ is hydrolyzed, and the A-ring is aromatized to provide better solubility in lipids, making the GA₃ derivatives promising drug leads (Cross et al. 1961).

Here, to investigate GA₃ derivatives with potential antitumor activities, we studied the ring-distortion of GA₃ under different conditions, and the yielded products were modified by amidation or substitution (Scheme 1). In the amidation route (Scheme 1a), the γ-lactone was hydrolyzed to allow aromatization, and the C- and D-rings of GA₃ experienced Wagner–Meerwein rearrangement to form **2** (Cross et al. 1961); then, it was reacted with a variety of primary amines **2** to form amide derivatives (**3a–3j**); finally, these derivatives were further underwent Baeyer–Villiger oxidation

Fig. 1 The chemical structure of GA₃ and representative tetracyclic diterpenes with antitumor activities (Egbewande et al. 2018; Liu et al. 2017; He et al. 2009; Sun et al. 1992)





Scheme 1 Preparation of GA₃ derivatives. **a** The synthetic route of amide derivatives series. **b** The synthetic route of ester derivatives series

rearrangement to produce amide derivatives (**4a–4b**). In the substitution route (Scheme **1b**), GA₃ was reacted under less acidic conditions to allow formation of **5**, and the C- and D-rings were preserved (Mulholland 1958). After this, substituted benzyl bromides were reacted with **5** to form ester derivatives (**6a–6j**) (Mo and Dong 2014), and oxidative rearrangement of these derivatives was carried out using 2,3-dichloro-5,6-dicyano-1,4-benzoquinone (DDQ), yielding ester derivatives (**7a–7j**) (Cross and Markwell 1973). After the chemical structure of these derivatives had been determined, we evaluated antitumor activities using MTT assay and ELISA.

Results and discussion

Chemistry

Aiming at finding GA₃ derivatives for promising antitumor activity, we designed two synthetic routes and received four series of products. In both routes, the configuration of tetracyclic diterpene structure was simplified in all GA₃ derivatives through the aromatization of the A-ring structure. As reported, the introducing of an amide side chain could influence the affinity with tyrosine kinase (Mandal et al. 2009; Chen et al. 2013), so here the amination route was designed. In this route, primary amines with different substituents group (i.e., acyclic alkyl groups with various chain length, cycloalkyl groups, and aromatic groups) were chosen to study the steric effect on the activity of GA₃ derivatives. In the second route, aromatic substituents with electron-drawing groups (including halogens, nitril, nitrile, and trifluoromethyl) and electron-donating groups (methyl, ethyl,

methoxyl, and phenoxy) were involved to explore the influence of the electronic effect on the activity of derivatives. This route was designed to identify whether halogens can enhance antitumor activities as observed on other GA₃ derivatives by Egbewande (Egbewande et al. 2018). Ester derivatives obtained were bridge-ring hexanones with two β , γ - carbon–carbon double bonds, while amide derivatives did not have these double bonds. The chemical structure of three series of derivatives are shown in Scheme 1.

These chemicals were analyzed by ¹H-NMR, ¹³C-NMR, high-resolution mass spectrometer (HRMS), FTIR and polarimetry (see Supplementary Data). Moreover, due to the complex spatial configurations, we further determined the configuration of derivatives **3c** and **7d** by single crystal X-ray diffraction (SXRD). Results shows that the unit cell of **3c** crystal was monoclinic and the space group was P2₁; the unit cell of **7d** crystal was orthorhombic and the space group was P2₁2₁2₁ (Fig. 2). According to these results, the spatial configurations of GA₃ derivatives were confirmed.

Evaluation of antitumor activity

One purpose of this research is to investigate the influence of the chemical structure of GA₃ derivatives on the antitumor activities. So, MTT assay was used to evaluate the inhibitory activity of GA₃ derivatives (22 in total) against the propagation of four kinds of cancer cells (Kim et al. 2001; Cao et al. 2004), including human promyelocytic acute leukemia cells (HL-60), human colon cancer cells (SW480), human breast cancer cells (MCF-7), and human lung squamous carcinoma cells (NCI-H226) (Xie et al. 2018). The results of MTT assay were indicated in Fig. 3 and Table 1.

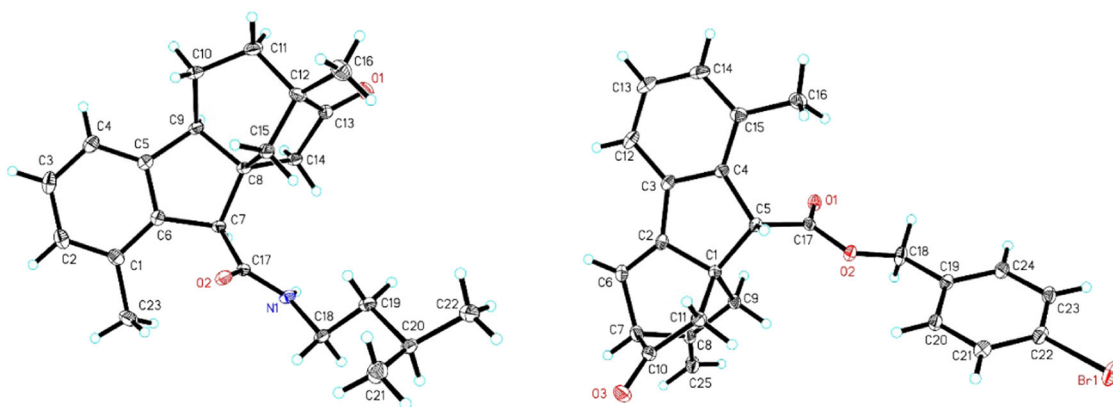


Fig. 2 The crystal structure of GA₃ derivatives **3c** and **7d** as determined by XRD

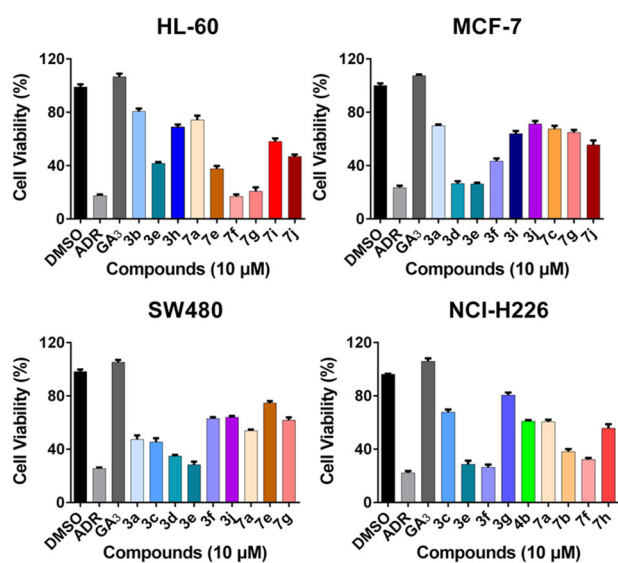


Fig. 3 Inhibitory activities of screened GA₃ derivatives (10 μM) against four tumor cell lines as determined by MTT assay. ADR adriamycin (positive control). GA₃ gibberellic acid. DMSO dimethylsulfoxide. Data were shown as mean ± SD ($n = 3$)

As shown in Fig. 3, at a concentration of 10 μM, most derivatives had a higher antitumor activity compared with that of GA₃. For MCF-7 and SW480, the antitumor activity of amide derivatives (**3a–3j**) were higher than that of ester derivatives (**7a–7j**). However, these ester derivatives displayed better activity against HL-60, and amide derivatives (**4a–4b**) showed lower activity against all four types of tumor cells.

As displayed in Table 1, compounds **3d**, **3e**, **3f**, **7e**, **7f**, and **7g** showed better inhibitory activity. More specifically, compound **3e** exhibited excellent activities against all four human tumor cell lines (IC₅₀ value 2.65–6.37 μM), and **3d** and **3f** exhibited potent activities against MCF-7 and SW480 cell lines (IC₅₀ value 3.23–8.23 μM). However, the

Table 1 Inhibitory activities of GA₃ derivatives against four tumor cells as determined by MTT assay

Compound	Cell line			
	HL-60	MCF-7	SW480	NCI-H226
3a	>50	26.41 ± 10.15	3.75 ± 0.36	>50
3b	40.56 ± 1.75	>50	>50	>50
3c	>50	>50	4.31 ± 0.41	44.42 ± 2.94
3d	>50	3.23 ± 0.19	6.13 ± 0.21	>50
3e	6.37 ± 0.14	4.01 ± 0.92	2.65 ± 0.50	5.60 ± 0.19
3f	>50	7.96 ± 0.69	8.23 ± 0.37	3.87 ± 0.53
3g	>50	>50	>50	>50
3h	38.95 ± 8.36	>50	>50	>50
3i	>50	46.32 ± 1.10	>50	>50
3j	>50	42.61 ± 0.88	42.02 ± 1.07	>50
4a	>50	>50	>50	>50
4b	>50	>50	>50	43.66 ± 3.05
7a	44.62 ± 2.13	>50	29.11 ± 1.26	41.57 ± 1.52
7b	>50	>50	>50	5.54 ± 0.34
7c	>50	45.24 ± 3.48	>50	>50
7d	>50	>50	>50	>50
7e	6.29 ± 1.55	>50	24.28 ± 9.19	>50
7f	4.21 ± 0.92	>50	>50	5.53 ± 0.46
7g	4.98 ± 0.21	44.87 ± 3.34	39.69 ± 3.90	>50
7h	>50	>50	>50	34.26 ± 2.73
7i	8.65 ± 0.59	>50	>50	>50
7j	6.29 ± 0.20	34.88 ± 3.44	>50	>50
GA ₃	>50	>50	>50	>50
ADR	0.86 ± 0.27	2.90 ± 0.36	2.88 ± 0.46	3.95 ± 0.61

Bold values mean the IC₅₀ lower than 10 μM. And these lower values deserve 50 more attention

IC₅₀, mean ± SD, μM

ester derivatives (**7e–7g** and **7i–7j**) were more selective to HL-60 cell lines with IC₅₀ value of 4.21–8.65 μM. Ester derivatives (**7a–7j**) did not show significant activity against

SW480 and MCF-7. On the other hand, derivatives **3e**, **3f**, **7b**, and **7f** gave better activities against NCI-H226 cell lines (IC_{50} value 3.87–5.60 μ M).

From the MTT assay, it can be found that amide derivatives with a saturated linear amide displayed better activity than those with an aromatic amide, especially when SW480 and NCI-H226 were involved. This result is similar as what has been reported by Chen et al., and the explanation can be that a amide with a long saturated alkyl chain could help improve the compound's affinity with kinases, thereby enhancing its inhibitory effect on cancer cells (Chen et al. 2013). The activities of **4a** and **4b** are generally lower than that of **3a** and **3j**, indicating that the bridge-ring heptanone structure could better contribute to the activity than the bridge-ring caprylolactone structure. Wu et al. as well as Egbewande et al. have reported that the introducing of electron-withdrawing groups (typically halogens) on the aromatic substitutes can strengthen the antitumor activity of some GA_3 derivatives (Wu et al. 2018; Egbewande et al. 2018). In our study, it was found that the benzyl group can improve the activity as well, and this might possibly be due to the interaction between the derivative and specific binding sites of the tumor cells. Meanwhile, ester derivatives (**7a–7j**) with a *meta*-substituted benzyl group showed better activities than those with a *para*-substituted benzyl group, and the difference in activity was more obvious when HL-60 was involved. Therefore, we had chosen derivatives that were more active, i.e., **3d**, **3e**, **3f**, **7e**, **7f** and **7g**, to study their inhibitory activity against the receptor protein–tyrosine kinases (RPTKs).

Inhibitory activity against four RPTKs

RPTK is an enzyme that plays an important role in regulating the growth, propagation, and differentiation of cells. Thus, it has become an important target of many types of cancer cells, and numerous new inhibitors targeting at this enzyme have been developed as anticancer drugs (Kassab and Hassan 2018). To identify whether the antitumor activity of GA_3 derivatives we prepared was related to the activation and expression of RPTKs receptor, ELISA was employed to evaluate the inhibitory activity of aforementioned six derivatives on four RPTKs, namely FGFR₁, ErbB₂, ALK, and KDR enzymes. As seen in Fig. 4, ester derivatives **7e**, **7f** and **7g** had a significant inhibitory activity against FGFR₁ and KDR enzymes, while amide derivatives **3d**, **3e** and **3f** did not show obvious impact. So, the inhibitory activity of ester derivatives might possibly be related to the inhibition of FGFR₁ activation and KDR activation, while amide derivatives may limit the propagation of tumor cells by other mechanisms.

Conclusion

In this research, two synthetic routes were designed and four series of new GA_3 rearrangement derivatives were obtained. The chemical structure of all GA_3 derivatives were identified by various analysis methods including ¹H-NMR, ¹³C-NMR, HRMS, FTIR and polarimetry, and the stereo configuration of **3c** and **7d** were determined by SXRD.

The antitumor activity of these three series of derivatives were initially evaluated by using four types of tumor cells (i.e., HL-60, SW480, MCF-7, and NCI-H226). Results show that most derivatives had a higher antitumor activity compared with GA_3 . When HL-60 was used, the inhibitory activities of ester derivatives (**7a–7j**) were higher than that of amide derivatives (**3a–3j**, **4a–4b**). All series had inhibitory activity against NCI-H226, though the activity of amide (**4a**, **4b**) was lower than that of amide (**3a–3j**). Considering the structure–function relationship, among amide derivatives, derivatives with a saturated linear amide had better activity than those with an aromatic amide, in particular when SW480 and NCI-H226 were involved. Among ester derivatives, those with a *meta*-substituted benzyl group showed higher activities than those with a *para*-substituted benzyl group, especially when HL-60 was applied. According to ELISA results, the antitumor activity of ester derivatives (**7a–7j**) were likely to be linked with the inhibition of FGFR₁ activation and KDR activation.

Overall, this research provides an initial study on how the antitumor activity of GA_3 was formed, and the structure–function relationship as revealed by this project would be helpful for the future design of more bioactive GA_3 derivatives.

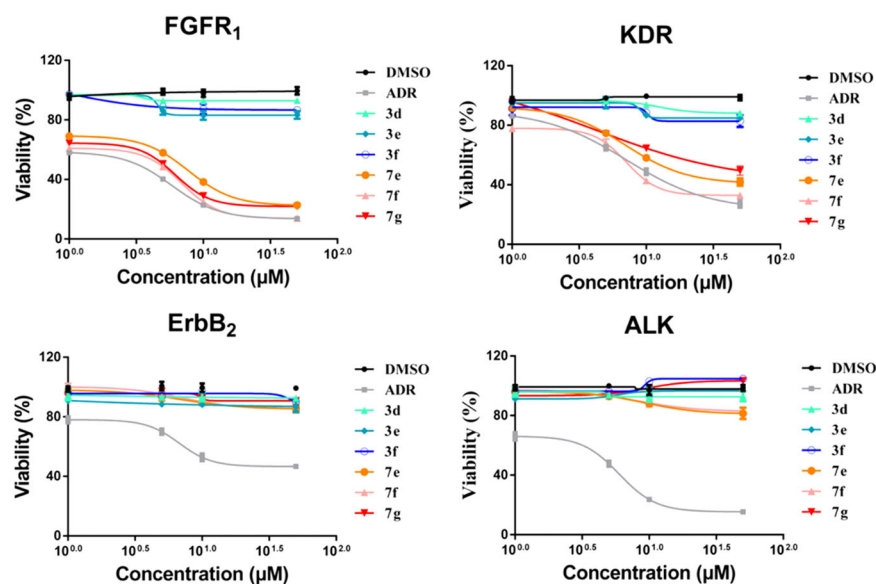
Materials and methods

Chemistry

Materials

All starting materials and reagents were obtained from Sigma-Aldrich, Energy Chemical, Aladdin or Innochem and were used as received. ¹H-NMR spectrums were obtained on a Bruker Avance 400 spectrometer at 400 MHz, and ¹³C-NMR spectra were recorded on the same spectrometer at 100 MHz. HRMS analyses were performed using a KE375 Pulsar mass spectrometer. FTIR spectrums were recorded using a Thermo Scientific Nicolet iS50 spectrometer. Optical rotations were measured on an Anton Paar MCP 5300 polarimeter. Thin layer chromatography was carried out on aluminum sheets coated with silica gel (silica HSGF254, Qingdao Marine Chemical

Fig. 4 The influence of concentration on the inhibitory activity against four types of RPTKs, as determined by ELISA assay. ADR adriamycin (as a positive control). DMSO: dimethylsulfoxide. Data were shown as mean \pm SD ($n = 3$)



Company, China). Column chromatography was carried out using a column of silica gel (200–300 mesh, Qingdao Marine Chemical Company, China). The analytical results are also available in Supplementary Information file.

Specific chemical transformations

(4*bS*,7*S*,9*aS*,10*R*)-1,7-Dimethyl-8-oxo-4*b*,6,7,8,9,10-hexahydro-5*H*-7,9*a*-methanobenzo[*a*]azulene-10-carboxylic acid (**2**). Gibberellic acid (1.92 g, 5.54 mmol) was suspended in aqueous hydrochloric acid (2.4 M, 250 mL) in a round bottom flask equipped with a reflux condenser. The reaction mixture was refluxed for 3 h at 100 °C. After reaction, the mixture was cooled down to the room temperature and then extracted with EtOAc (3 \times 200 mL). The combined organic layer was washed with brine (2 \times 300 mL), dried over anhydrous Na₂SO₄ and concentrated in a vacuum. The residue was subjected to column chromatography (PE/EtOAc = 3:1) to afford product **2** as a white solid (1.20 g, 76.5%). ¹H-NMR (400 MHz, CDCl₃): δ 7.24 (t, $J = 7.5$ Hz, 1 H), 7.08 (d, $J = 7.5$ Hz, 1 H), 6.99 (d, $J = 7.5$ Hz, 1 H), 4.68 (s, 1 H), 3.03 (t, $J = 7.6$ Hz, 1H), 2.92 (d, $J = 17.8$ Hz, 1 H), 2.57 (dd, $J = 17.8, 3.7$ Hz, 1 H), 2.25 (s, 3 H), 2.17–2.08 (m, 1 H), 2.05 (dd, $J = 11.9, 3.5$ Hz, 1 H), 1.95–1.85 (m, 1 H), 1.81–1.71 (m, 1 H), 1.69–1.59 (m, 1 H), 1.55 (d, $J = 12.0$ Hz, 1 H), 1.09 (s, 3 H). ¹³C-NMR (100 MHz, CDCl₃): δ 173.0, 145.4, 136.7, 135.3, 129.3, 129.1, 120.6, 67.1, 51.5, 50.8, 50.1, 48.0, 38.5, 34.2, 22.9, 21.5, 20.2. FTIR (MeOH): $\nu_{\max} = 3356, 2923, 2866, 1739, 1634, 1455, 1336, 1261, 1196, 1159, 1021$ cm⁻¹. HRMS (ESI): m/z calcd for C₁₈H₂₀O₃Na [M + Na]⁺: 307.1310, found: 307.1308.

General procedure for the preparation of (4*bS*,7*S*,9*aS*,10*R*)-*N*-substituted-1,7-dimethyl-8-oxo-4*b*,6,7,8,9,10-hexahydro-5*H*-7,9*a*-methanobenzo[*a*]azulene-10-carboxamide (**3a–3j**).

Under an argon atmosphere, **2** (600 mg, 2.11 mmol) was dissolved in dry tetrahydrofuran (50 mL) in an oven-dried round bottom flask. After thionyl chloride (4.64 mmol, 2.2 eq) was added, the reaction mixture was refluxed for 1 h and then cooled in an ice bath. After that, triethylamine (680 μ L, 4.85 mmol) and the amine (7.17 mmol, 3.4 eq) was added. The reaction mixture was allowed to warm to room temperature for 1 h, and then the reaction was quenched with water (50 mL). After extracted with EtOAc (3 \times 50 mL), the combined organic layer was washed with brine (2 \times 100 mL), dried over anhydrous Na₂SO₄ and concentrated in a vacuum. The residue was subjected to column chromatography (PE/EtOAc = 4:1–3:1) to afford derivatives **3a–3j**.

(4*bS*,7*S*,9*aS*,10*R*)-*N*-butyl-1,7-dimethyl-8-oxo-4*b*,6,7,8,9,10-hexahydro-5*H*-7,9*a*-methanobenzo[*a*]azulene-10-carboxamide (**3a**). Yield: 52.3% as a white solid. [α]_D²⁵ = +35.3 ($c = 1.0$, CH₃OH). ¹H-NMR (400 MHz, DMSO-*d*₆): δ 7.12 (t, $J = 7.4$ Hz, 1 H), 6.97 (dd, $J = 7.4, 5.5$ Hz, 2 H), 3.96 (s, 1 H), 3.14 (q, $J = 6.5$ Hz, 2 H), 2.92 (t, $J = 8.0$ Hz, 1 H), 2.52 (d, $J = 12.8$ Hz, 1 H), 2.42 (dd, $J = 17.9, 3.4$ Hz, 1 H), 2.09 (s, 3 H), 1.99 (dd, $J = 6.9, 1.7$ Hz, 1 H), 1.89 (dd, $J = 12.2, 3.3$ Hz, 1 H), 1.77–1.66 (m, 1 H), 1.61–1.50 (m, 2 H), 1.50–1.39 (m, 2 H), 1.37–1.25 (m, 3 H), 1.17 (d, $J = 12.3$ Hz, 1 H), 0.93 (s, 3 H), 0.88 (t, $J = 7.3$ Hz, 3 H). ¹³C-NMR (100 MHz, DMSO-*d*₆): δ 219.7, 171.1, 147.5, 140.8, 135.8, 129.3, 128.3, 121.3, 57.4, 51.8, 51.6, 50.1, 48.3, 39.5, 35.0, 32.3, 23.8, 22.7, 20.8, 20.0, 19.5, 14.8. FTIR (MeOH): $\nu_{\max} = 3288, 2956, 2928, 2865, 1738, 1642, 1545, 1455, 1374, 1239, 1082$ cm⁻¹. HRMS (ESI): m/z calcd for C₂₂H₃₀NO₂ [M + H]⁺: 340.2271, found: 340.2269.

(4*bS*,7*S*,9*aS*,10*R*)-*N*-isobutyl-1,7-dimethyl-8-oxo-4*b*,6,7,8,9,10-hexahydro-5*H*-7,9*a*-methanobenzo[*a*]azulene-10-carboxamide (**3b**). Yield: 68.7% as a white solid.

$[\alpha]_D^{25} = +33.7$ ($c = 1.0$, CH_3OH). $^1\text{H-NMR}$ (400 MHz, $\text{DMSO-}d_6$): δ 7.12 (t, $J = 7.5$ Hz, 1 H), 6.97 (t, $J = 6.9$ Hz, 2 H), 4.00 (s, 1 H), 2.97 (t, $J = 6.5$ Hz, 2 H), 2.58 (d, $J = 18.0$ Hz, 1 H), 2.54–2.47 (m, 1 H), 2.44 (dd, $J = 18.0$, 3.4 Hz, 1 H), 2.09 (s, 3 H), 2.06–1.96 (m, 1 H), 1.88 (dd, $J = 12.4$, 3.3 Hz, 1 H), 1.81–1.66 (m, 2 H), 1.60–1.50 (m, 2 H), 1.16 (d, $J = 12.4$ Hz, 1 H), 0.92 (s, 3 H), 0.88 (dd, $J = 6.6$, 1.6 Hz, 6 H). $^{13}\text{C-NMR}$ (100 MHz, $\text{DMSO-}d_6$) δ 219.4, 170.9, 147.2, 140.5, 135.5, 129.0, 128.0, 121.0, 57.1, 51.5, 51.3, 49.9, 48.0, 47.4, 39.5, 34.7, 28.7, 23.5, 22.5, 21.2, 21.1, 19.7. FTIR (MeOH): $\nu_{\text{max}} = 3293, 2956, 2868, 1739, 1644, 1545, 1465, 1372, 1239, 1160, 1016 \text{ cm}^{-1}$. HRMS (ESI): m/z calcd for $\text{C}_{22}\text{H}_{30}\text{NO}_2$ $[\text{M} + \text{H}]^+$: 340.2277, found: 340.2277. m/z calcd for $\text{C}_{22}\text{H}_{29}\text{NO}_2\text{Na}$ $[\text{M} + \text{Na}]^+$: 362.2096, found: 362.2096.

(4*bS*,7*S*,9*aS*,10*R*)-*N*-isopentyl-1,7-dimethyl-8-oxo-4*b*,6,7,8,9,10-hexahydro-5*H*-7,9*a*-methanobenzo[*a*]azulene-10-carboxamide (**3c**). Yield: 50.1% as a colorless crystalline solid. $[\alpha]_D^{25} = +31.8$ ($c = 1.0$, CH_3OH). $^1\text{H-NMR}$ (400 MHz, CDCl_3): δ 7.53 (t, $J = 7.5$ Hz, 1 H), 7.30 (d, $J = 7.2$ Hz, 1 H), 7.20 (d, $J = 6.7$ Hz, 1 H), 3.03 (dd, $J = 12.1$, 6.8 Hz, 1 H), 2.90 (d, $J = 17.8$ Hz, 1 H), 2.70 (s, 3 H), 2.26 (ddd, $J = 13.7, 9.5, 5.1$ Hz, 2 H), 2.01 (dd, $J = 11.9, 3.7$ Hz, 1 H), 1.93–1.84 (m, 1 H), 1.77 (dd, $J = 14.3, 7.8$ Hz, 1 H), 1.73–1.67 (m, 2 H), 1.65–1.56 (m, 2 H), 1.47–1.41 (m, 2 H), 1.30–1.25 (m, 4 H), 1.16 (s, 3 H), 1.13 (s, 4 H). $^{13}\text{C-NMR}$ (100 MHz, DMSO) δ 218.9, 171.0, 147.5, 140.7, 135.7, 129.3, 128.3, 121.2, 57.4, 51.7, 51.5, 50.1, 48.2, 47.6, 39.6, 39.2, 38.0, 34.9, 26.2, 23.8, 23.5, 22.7, 19.9. FTIR (MeOH): $\nu_{\text{max}} = 3295, 2955, 2930, 2868, 1740, 1645, 1545, 1454, 1368, 1240, 1084, 1015, 769 \text{ cm}^{-1}$. HRMS (ESI): m/z calcd for $\text{C}_{23}\text{H}_{32}\text{NO}_2$ $[\text{M} + \text{H}]^+$: 354.2428, found: 354.2426.

(4*bS*,7*S*,9*aS*,10*R*)-*N*-hexyl-1,7-dimethyl-8-oxo-4*b*,6,7,8,9,10-hexahydro-5*H*-7,9*a*-methanobenzo[*a*]azulene-10-carboxamide (**3d**). Yield: 80.6% as a colorless crystalline solid. $[\alpha]_D^{25} = +31.6$ ($c = 2.0$, CH_3OH). $^1\text{H-NMR}$ (400 MHz, CDCl_3): δ 7.21 (t, $J = 5.6$ Hz, 1 H), 7.03 (d, $J = 6.8$ Hz, 2 H), 4.01 (s, 1 H), 3.34–3.24 (m, 2 H), 2.92 (t, $J = 7.9$ Hz, 1 H), 2.70 (d, $J = 17.4$ Hz, 1 H), 2.23 (s, 3 H), 2.02 (dd, $J = 12.1, 3.1$ Hz, 1 H), 1.91–1.60 (m, 4 H), 1.52 (d, $J = 6.3$ Hz, 2 H), 1.45 (t, $J = 6.8$ Hz, 2 H), 1.36–1.25 (m, 6 H), 1.06 (s, 3 H), 0.94–0.88 (m, 3 H). $^{13}\text{C-NMR}$ (100 MHz, CDCl_3): δ 217.3, 171.5, 147.1, 138.5, 135.5, 129.5, 128.6, 121.1, 58.1, 51.7, 51.0, 49.7, 48.2, 40.0, 38.9, 34.7, 31.9, 30.0, 27.2, 23.6, 23.0, 22.0, 19.7, 14.4. FTIR (MeOH): $\nu_{\text{max}} = 3290, 2955, 2928, 2861, 1740, 1644, 1545, 1455, 1374, 1240, 1082, 1030, 770, 716 \text{ cm}^{-1}$. HRMS (ESI): m/z calcd for $\text{C}_{24}\text{H}_{34}\text{NO}_2$ $[\text{M} + \text{H}]^+$: 368.2584, found: 368.2585.

(4*bS*,7*S*,9*aS*,10*R*)-*N*-octyl-1,7-dimethyl-8-oxo-4*b*,6,7,8,9,10-hexahydro-5*H*-7,9*a*-methanobenzo[*a*]azulene-10-carboxamide (**3e**). Yield: 80.2% as a white solid.

$[\alpha]_D^{25} = +24.9$ ($c = 2.0$, CH_3OH). $^1\text{H-NMR}$ (400 MHz, CDCl_3): δ 7.20 (t, $J = 7.5$ Hz, 1 H), 7.04 (d, $J = 7.4$ Hz, 1 H), 7.01 (d, $J = 7.5$ Hz, 1 H), 5.83 (br s, 1 H), 4.00 (s, 1 H), 3.28 (dd, $J = 13.6, 6.7$ Hz, 2 H), 2.92 (t, $J = 7.8$ Hz, 1 H), 2.70 (d, $J = 17.6$ Hz, 1 H), 2.39 (dd, $J = 17.7, 3.3$ Hz, 1 H), 2.23 (s, 3 H), 2.15–2.05 (m, 1 H), 1.98 (dd, $J = 12.1, 3.3$ Hz, 1 H), 1.88–1.71 (m, 2 H), 1.67–1.58 (m, 1 H), 1.45 (d, $J = 12.2$ Hz, 1 H), 1.33–1.21 (m, 12 H), 1.05 (s, 3 H), 0.88 (t, $J = 6.8$ Hz, 3 H). $^{13}\text{C-NMR}$ (100 MHz, CDCl_3): δ 219.4, 171.7, 143.7, 140.6, 135.7, 129.7, 128.2, 123.7, 58.6, 50.6, 48.3, 47.7, 44.2, 40.1, 34.7, 32.2, 29.9, 29.7, 29.6, 27.5, 23.0, 22.0, 21.7, 19.7, 19.1, 14.4. FTIR (MeOH): $\nu_{\text{max}} = 3291, 2926, 2856, 1740, 1644, 1544, 1455, 1375, 1240, 1018, 769, 715 \text{ cm}^{-1}$. HRMS (ESI): m/z calcd for $\text{C}_{26}\text{H}_{38}\text{NO}_2$ $[\text{M} + \text{H}]^+$: 396.2897, found: 396.2895.

(4*bS*,7*S*,9*aS*,10*R*)-*N*-(cyclohexylmethyl)-1,7-dimethyl-8-oxo-4*b*,6,7,8,9,10-hexahydro-5*H*-7,9*a*-methanobenzo[*a*]azulene-10-carboxamide (**3f**). Yield: 59.1% as a white solid. $[\alpha]_D^{25} = +33.8$ ($c = 1.0$, CH_3OH). $^1\text{H-NMR}$ (400 MHz, CDCl_3): δ 7.21 (t, $J = 7.5$ Hz, 1 H), 7.06 (d, $J = 7.4$ Hz, 1 H), 7.01 (d, $J = 7.5$ Hz, 1 H), 5.58 (br s, 1 H), 4.00 (s, 1 H), 3.13 (t, $J = 6.3$ Hz, 2 H), 2.94 (t, $J = 7.8$ Hz, 1 H), 2.71 (d, $J = 17.5$ Hz, 1 H), 2.43 (dd, $J = 17.6, 3.5$ Hz, 1 H), 2.22 (s, 3 H), 2.14–2.04 (m, 1 H), 1.95 (dd, $J = 12.0, 3.4$ Hz, 1 H), 1.83–1.62 (m, 10 H), 1.46 (d, $J = 11.8$ Hz, 2 H), 1.23–1.12 (m, 3 H), 1.05 (s, 3 H). $^{13}\text{C-NMR}$ (100 MHz, CDCl_3): δ 218.7, 185.2, 137.8, 135.4, 129.3, 128.5, 120.9, 100.0, 58.2, 51.7, 51.3, 47.9, 46.0, 38.5, 37.8, 34.3, 31.1, 31.1, 26.3, 25.7, 25.7, 25.6, 23.3, 21.6, 19.3. FTIR (MeOH): $\nu_{\text{max}} = 3291, 3072, 2923, 2852, 1741, 1644, 1550, 1450, 1373, 1278, 1240, 1082, 990, 770, 716 \text{ cm}^{-1}$. HRMS (ESI): m/z calcd for $\text{C}_{25}\text{H}_{34}\text{NO}_2$ $[\text{M} + \text{H}]^+$: 380.2584, found: 380.2579.

(4*bS*,7*S*,9*aS*,10*R*)-*N*-phenyl-1,7-dimethyl-8-oxo-4*b*,6,7,8,9,10-hexahydro-5*H*-7,9*a*-methanobenzo[*a*]azulene-10-carboxamide (**3g**). Yield: 54.2% as a white solid. $[\alpha]_D^{25} = +34.5$ ($c = 1.0$, CH_3OH). $^1\text{H-NMR}$ (400 MHz, CDCl_3): δ 7.39 (d, $J = 7.6$ Hz, 2 H), 7.24–7.14 (m, 3 H), 7.03 (dt, $J = 12.7, 6.5$ Hz, 3 H), 4.14 (s, 1 H), 2.89 (t, $J = 7.5$ Hz, 1 H), 2.68 (dd, $J = 17.7, 3.7$ Hz, 1 H), 2.48–2.31 (m, 1 H), 2.23 (s, 3 H), 2.11–1.98 (m, 2 H), 1.88–1.65 (m, 1 H), 1.57 (dd, $J = 13.3, 7.4$ Hz, 1 H), 1.46 (d, $J = 11.6$ Hz, 1 H), 1.25 (d, $J = 7.1$ Hz, 1 H), 0.97 (s, 3 H). $^{13}\text{C-NMR}$ (100 MHz, CDCl_3): δ 219.2, 169.9, 147.1, 137.3, 135.4, 129.5, 129.1, 128.8 ($\times 2$), 128.1, 124.8, 121.1, 120.3 ($\times 2$), 58.9, 51.4, 49.9, 47.9, 38.3, 34.3, 29.7, 23.3, 21.6, 19.3. FTIR (MeOH): $\nu_{\text{max}} = 3305, 2930, 2838, 1737, 1661, 1599, 1540, 1499, 1442, 1305, 1249, 1115, 1017, 754, 692, 576 \text{ cm}^{-1}$. HRMS (ESI): m/z calcd for $\text{C}_{24}\text{H}_{26}\text{NO}_2$ $[\text{M} + \text{H}]^+$: 360.1958, found: 360.1965.

(4*bS*,7*S*,9*aS*,10*R*)-*N*-benzyl-1,7-dimethyl-8-oxo-4*b*,6,7,8,9,10-hexahydro-5*H*-7,9*a*-methanobenzo[*a*]azulene-10-carboxamide (**3h**). Yield: 68.1% as a white solid. $[\alpha]_D^{25} = +19.7$ ($c = 1.0$, CH_3OH). $^1\text{H-NMR}$ (400 MHz,

CDCl₃): δ 7.41–7.31 (m, 5 H), 7.25 (t, J = 7.5 Hz, 1 H), 7.07 (dd, J = 13.1, 7.5 Hz, 2 H), 5.90 (br s, 1 H), 4.53 (d, J = 5.5 Hz, 2 H), 4.09 (s, 1 H), 2.98 (t, J = 7.8 Hz, 1 H), 2.76 (d, J = 17.6 Hz, 1 H), 2.47 (d, J = 17.8 Hz, 1 H), 2.23 (s, 3 H), 2.18–2.06 (m, 1 H), 1.94 (dd, J = 12.0, 3.5 Hz, 1 H), 1.88–1.76 (m, 2 H), 1.71–1.63 (m, 1 H), 1.46 (d, J = 11.8 Hz, 1 H), 1.07 (s, 3 H). ¹³C-NMR (100 MHz, CDCl₃): δ 219.3, 171.1, 146.7, 138.3, 135.1, 129.0, 128.5, 128.2 (\times 2), 128.1 (\times 2), 127.5, 127.4, 120.6, 60.4, 57.5, 51.2, 49.6, 47.8, 43.6, 38.6, 34.3, 23.0, 21.5, 19.4. FTIR (MeOH): ν_{\max} = 3286, 3065, 2927, 2865, 1738, 1648, 1598, 1545, 1454, 1402, 1240, 1082, 1027, 800, 728, 699, 610, 552 cm⁻¹. HRMS (ESI): m/z calcd for C₂₅H₂₈NO₂ [M + H]⁺: 374.2115, found: 374.2120.

(4*b*S,7*S*,9*a*S,10*R*)-*N*-(4-chlorobenzyl)-1,7-dimethyl-8-oxo-4*b*,6,7,8,9,10-hexahydro-5*H*-7,9*a*-methanobenzo[*a*]azulene-10-carboxamide (**3i**). Yield: 51.0% as a white solid. $[\alpha]_{\text{D}}^{25}$ = +18.3 (c = 1.0, CH₃OH). ¹H-NMR (400 MHz, CDCl₃): δ 7.34 (d, J = 8.6 Hz, 2 H), 7.29 (d, J = 8.1 Hz, 2 H), 7.25 (d, J = 7.6 Hz, 1 H), 7.09 (d, J = 7.7 Hz, 1 H), 7.05 (d, J = 7.6 Hz, 1 H), 6.00 (br s, 1 H), 4.49 (d, J = 5.8 Hz, 2 H), 4.08 (s, 1 H), 2.98 (t, J = 7.9 Hz, 1 H), 2.74 (d, J = 17.6 Hz, 1 H), 2.46 (dd, J = 17.6, 3.5 Hz, 1 H), 2.20 (s, 3 H), 2.14 (dd, J = 11.6, 5.9 Hz, 1 H), 1.92 (dd, J = 12.5, 3.7 Hz, 1 H), 1.84–1.74 (m, 2 H), 1.70–1.61 (m, 1 H), 1.40 (d, J = 12.0 Hz, 1 H), 1.07 (s, 3 H). ¹³C-NMR (100 MHz, CDCl₃): δ 171.5, 147.3, 137.7, 136.9, 135.6, 133.9, 130.1 (\times 2), 129.6, 129.1 (\times 2), 128.9, 121.2, 58.3, 51.9, 51.6, 49.7, 48.1, 43.4, 38.7, 34.5, 23.5, 21.8, 19.6. FTIR (MeOH): ν_{\max} = 3284, 3065, 2926, 2865, 1738, 1649, 1597, 1542, 1492, 1454, 1406, 1373, 1240, 1090, 1015, 800, 768, 716, 628 cm⁻¹. HRMS (ESI): m/z calcd for C₂₅H₂₇ClNO₂ [M + H]⁺: 408.1725, 410.1706, found: 408.1725, 410.1705 (3:1). m/z calcd for C₂₅H₂₆ClNO₂Na [M + Na]⁺: 430.1544, 432.1525, found: 430.1544, 432.1525 (3:1).

(4*b*S,7*S*,9*a*S,10*R*)-*N*-(4-bromobenzyl)-1,7-dimethyl-8-oxo-4*b*,6,7,8,9,10-hexahydro-5*H*-7,9*a*-methanobenzo[*a*]azulene-10-carboxamide (**3j**). Yield: 69.7% as a white solid. $[\alpha]_{\text{D}}^{25}$ = +7.28.3 Hz, 2 H), 7.22 (t, J = 7.5 Hz, 1 H), 7.18 (d, J = 8.3 Hz, 2 H), 7.04 (d, J = 7.5 Hz, 1 H), 7.00 (d, J = 7.6 Hz, 1 H), 6.04 (br s, 1 H), 4.42 (d, J = 5.9 Hz, 2 H), 4.03 (s, 1 H), 2.93 (t, J = 7.8 Hz, 1 H), 2.69 (d, J = 17.4 Hz, 1 H), 2.41 (dd, J = 17.7, 3.6 Hz, 1 H), 2.15 (s, 3 H), 2.08 (d, J = 11.4 Hz, 1 H), 1.87 (dd, J = 12.0, 3.6 Hz, 1 H), 1.83–1.68 (m, 2 H), 1.34 (d, J = 12.0 Hz, 1 H), 1.31–1.23 (m, 1 H), 1.02 (s, 3 H). ¹³C-NMR (100 MHz, CDCl₃): δ 171.4, 147.2, 137.7, 137.4, 135.5, 132.0 (\times 2), 130.4 (\times 2), 129.6, 128.8, 121.9, 121.2, 58.2, 51.9, 51.6, 49.7, 48.1, 43.4, 38.7, 34.5, 23.5, 21.8, 19.6. FTIR (MeOH): ν_{\max} = 3283, 3064, 2926, 2863, 1738, 1648, 1595, 1539, 1487, 1454, 1404, 1373, 1260, 1240, 1071, 1012, 798, 768, 716, 628, 536 cm⁻¹. HRMS (ESI): m/z calcd for C₂₅H₂₇BrNO₂ [M + H]⁺: 452.1220, 454.1203, found: 452.1221, 454.1196

(1:1). m/z calcd for C₂₅H₂₆BrNO₂Na [M + Na]⁺: 474.1039, 476.1022, found: 474.1040, 476.1025 (1:1).

General procedure for the preparation of (4*S*,6*a*S,11*R*,11*a*S)-*N*-substituted-4,10-dimethyl-2-oxo-1,2,5,6,6*a*,11-hexahydro-4*H*-4,11*a*-methanoindeno[2,1-*d*]oxocine-11-carboxamide (**4a–4b**). Under an argon atmosphere, derivative **3d** or **3g** (1.2 mmol, 1 eq) was dissolved in dichloromethane (30 mL) in a round bottom flask. After the mixture was cooled to 0 °C in an ice bath, sodium carbonate (1.02 g, 9.6 mmol, 8 eq) and *m*-chloroperoxybenzoic acid (414 mg, 2.4 mmol, 2 eq) were added. The reaction mixture was allowed to warm to room temperature and then stirred for 15 h (Krow 2004). The reaction mixture was quenched with saturated aqueous sodium bicarbonate (20 mL), then acidified to pH 3 by aqueous HCl. The aqueous layer was extracted with EtOAc (3 \times 20 mL). The combined organic layers were washed with brine (30 mL), dried over anhydrous Na₂SO₄, and concentrated in a vacuum. The residue was subjected to column chromatography (PE/EtOAc = 3:1 to 2:1) to afford amide derivatives **4a** or **4b**.

(4*S*,6*a*S,11*R*,11*a*S)-*N*-phenyl-4,10-dimethyl-2-oxo-1,2,5,6,6*a*,11-hexahydro-4*H*-4,11*a*-methanoindeno[2,1-*d*]oxocine-11-carboxamide (**4a**). Yield: 41.6% as a white solid. $[\alpha]_{\text{D}}^{25}$ = -55.5 (c = 1.0, CH₃OH). ¹H-NMR (400 MHz, CDCl₃): δ 7.42 (d, J = 8.0 Hz, 2 H), 7.30–7.17 (m, 3 H), 7.07 (t, J = 8.2 Hz, 2 H), 7.01 (d, J = 7.9 Hz, 1 H), 4.12 (s, 1 H), 2.93 (t, J = 8.1 Hz, 1 H), 2.73 (d, J = 17.8 Hz, 1 H), 2.41 (dd, J = 17.5, 3.8 Hz, 1 H), 2.23 (s, 3 H), 2.15–2.00 (m, 1 H), 1.77 (ddt, J = 22.0, 16.5, 5.3 Hz, 2 H), 1.64–1.52 (m, 2 H), 1.49 (d, J = 12.3 Hz, 1 H), 0.98 (s, 3 H). ¹³C-NMR (100 MHz, CDCl₃): δ 169.6, 168.3, 145.1, 138.3, 136.9, 135.1, 134.8, 129.2, 128.8, 128.7, 128.5, 124.5, 120.7, 119.9, 58.7, 51.1, 49.5, 47.6, 36.3, 34.0, 22.1, 21.3, 19.4, 19.0. FTIR (MeOH): ν_{\max} = 3300, 3040, 2926, 2865, 1738, 1660, 1599, 1538, 1499, 1441, 1401, 1360, 1305, 1247, 1173, 1081, 1030, 754, 693, 573 cm⁻¹. HRMS (ESI): m/z calcd for C₂₄H₂₆NO₃ [M + H]⁺: 376.1907, found: 376.1910.

(4*S*,6*a*S,11*R*,11*a*S)-*N*-hexyl-4,10-dimethyl-2-oxo-1,2,5,6,6*a*,11-hexahydro-4*H*-4,11*a*-methanoindeno[2,1-*d*]oxocine-11-carboxamide (**4b**). Yield: 74.8% as a white solid. $[\alpha]_{\text{D}}^{25}$ = -39.0 (c = 1.0, CH₃OH). ¹H-NMR (400 MHz, CDCl₃): δ 7.19 (s, 1 H), 7.15 (d, J = 3.2 Hz, 1 H), 7.04 (d, J = 3.8 Hz, 1 H), 6.55 (br s, 1 H), 4.05 (q, J = 7.4 Hz, 1 H), 3.62 (d, J = 17.6 Hz, 1 H), 3.49 (s, 1 H), 3.40 (s, 1 H), 3.26 (dq, J = 13.5, 6.8 Hz, 1 H), 3.17 (dt, J = 13.3, 6.1 Hz, 1 H), 2.78 (d, J = 17.7 Hz, 1 H), 2.37 (d, J = 13.9 Hz, 1 H), 1.96 (s, 3 H), 1.62 (d, J = 12.7 Hz, 2 H), 1.51–1.40 (m, 2 H), 1.32–1.15 (m, 9 H), 1.11 (s, 2 H), 0.83 (t, J = 5.9 Hz, 3 H). ¹³C-NMR (100 MHz, CDCl₃): δ 176.3, 168.1, 139.7, 138.8, 135.4, 131.6, 127.3, 120.2, 94.3, 68.7, 59.4, 52.4, 51.5, 39.8, 38.8, 36.7, 33.4, 31.3, 30.4, 28.3,

25.6, 21.6, 18.1, 13.0. FTIR (MeOH): ν_{\max} = 3318, 2928, 2857, 1745, 1653, 1546, 1460, 1376, 1289, 1239, 1118, 1049, 984, 938, 783, 737, 705, 640, 551 cm^{-1} . HRMS (ESI): m/z calcd for $\text{C}_{24}\text{H}_{34}\text{NO}_3$ $[\text{M} + \text{H}]^+$: 384.3533, found: 384.3528. m/z calcd for $\text{C}_{24}\text{H}_{33}\text{NO}_3\text{Na}$ $[\text{M} + \text{Na}]^+$: 406.2353, found: 406.2351.

(4*b*R,7*S*,9*a*S,10*R*)-7-Hydroxy-1-methyl-8-methylene-4*b*,6,7,8,9,10-hexahydro-5*H*-7,9*a*-methanobenzo[*a*]azulene-10-carboxylic acid (**5**). Gibberellic acid (2.80 g, 8.10 mmol) was dissolved in hydrochloric acid (1.2 M, 40 mL) in a round bottom flask equipped with a magnetic stirrer. The reaction was carried out for 3 h at 65 °C. Then, the reaction mixture was cooled to room temperature. The white solid precipitate was collected by filtration and washed with cold water (3 × 20 mL). The crude product was dissolved in boiling EtOAc and then precipitated after cooling in an ice bath for 1 h. The mixture was filtered and washed with cold EtOAc (3 × 10 mL) to provide product **5** as a white solid (1.79 g, 78.0%): $^1\text{H-NMR}$ (300 MHz, methanol-*d*₄): δ 7.10 (t, J = 7.5 Hz, 1 H), 6.98 (d, J = 7.5 Hz, 1 H), 6.91 (d, J = 7.2 Hz, 1 H), 5.02–4.99 (m, 1 H), 4.76 (s, 1 H), 3.89 (s, 1 H), 2.73 (dd, J = 19.7, 12.2 Hz, 1 H), 2.31–2.23 (m, 3 H), 2.21 (s, 3 H), 2.10–2.02 (m, 2 H), 1.94 (dd, J = 12.0, 5.0 Hz, 1 H), 1.86 (dd, J = 12.5, 7.7 Hz, 1 H), 1.73–1.64 (m, 1 H), 1.55 (ddd, J = 25.3, 12.6, 5.0 Hz, 1 H). $^{13}\text{C-NMR}$ (75 MHz, methanol-*d*₄): δ 174.5, 155.1, 145.4, 139.2, 135.6, 129.2, 127.8, 120.0, 103.1, 80.6, 55.4, 53.6, 52.6, 48.6, 40.1, 34.7, 22.5, 19.5. FTIR (MeOH): ν_{\max} = 3748, 3394, 2930, 2868, 1706, 1457, 1332, 1293, 1252, 1195, 1107, 1044, 886, 771 cm^{-1} . HRMS (ESI) m/z calcd for $\text{C}_{18}\text{H}_{19}\text{O}_3$ $[\text{M-H}]^-$: 283.1334, found: 283.1336.

General procedure for the preparation of substituted (7*S*,9*a*S,10*R*)-7-Hydroxy-1-methyl-8-methylene-4*b*,6,7,8,9,10-hexahydro-5*H*-7,9*a*-methanobenzo[*a*]azulene-10-carboxylate (**6a–6j**). Compound **5** (0.50 g, 1.76 mmol) and the benzyl bromide (4.40 mmol, 2.5 eq) was dissolved in acetone (10 mL) in an oven-dried round bottom flask with a magnetic stirring bar. After potassium carbonate (1.22 g, 8.79 mmol) was added, the reaction was carried out at room temperature for 16 h. Then, the reaction mixture was diluted with water (10 mL) and extracted with EtOAc (2 × 10 mL). The combined organic layer was washed with brine (2 × 20 mL), dried over anhydrous Na_2SO_4 and concentrated in a vacuum. The residue was purified by column chromatography on silica gel (PE/EtOAc = 4:1–3:1) to afford ester products **6a–6j**.

Benzyl(7*S*,9*a*S,10*R*)-7-hydroxy-1-methyl-8-methylene-4*b*,6,7,8,9,10-hexahydro-5*H*-7,9*a*-methanobenzo[*a*]azulene-10-carboxylate (**6a**). Yield: 87.9% as a yellow oily liquid. $^1\text{H-NMR}$ (400 MHz, CDCl_3): δ 13.25–13.19 (m, 1 H), 7.46 (d, J = 7.7 Hz, 2 H), 7.42 (s, 2 H), 7.39 (d, J = 4.2 Hz, 1 H), 7.20 (t, J = 7.5 Hz, 1 H), 7.06 (d, J = 7.6 Hz, 1 H), 6.99 (d, J = 7.3 Hz, 1 H), 5.33 (d, J = 12.2 Hz, 1 H),

5.24 (d, J = 12.3 Hz, 1 H), 5.10 (s, 1 H), 4.81 (s, 1 H), 4.05 (s, 1 H), 2.81 (dd, J = 12.3, 4.3 Hz, 1 H), 2.28 (d, J = 10.5 Hz, 2 H), 2.20 (s, 4 H), 2.09 (s, 1 H), 2.02 (dd, J = 12.3, 5.1 Hz, 1 H), 1.95 (d, J = 9.9 Hz, 1 H), 1.80 (d, J = 10.5 Hz, 1 H). $^{13}\text{C-NMR}$ (100 MHz, CDCl_3): δ 171.4, 154.3, 144.6, 138.4, 135.8, 135.0, 129.1, 128.7, 128.5, 127.5, 119.8, 103.5, 80.5, 66.7, 54.8, 53.6, 52.0, 48.7, 39.5, 34.2, 22.1, 20.0.

4-Nitrobenzyl (7*S*,9*a*S,10*R*)-7-hydroxy-1-methyl-8-methylene-4*b*,6,7,8,9,10-hexahydro-5*H*-7,9*a*-methanobenzo[*a*]azulene-10-carboxylate (**6b**). Yield: 85.3% as a white solid. $^1\text{H-NMR}$ (400 MHz, CDCl_3): δ 8.25 (d, J = 8.7 Hz, 2 H), 7.59 (d, J = 8.7 Hz, 2 H), 7.16 (t, J = 7.5 Hz, 1 H), 7.02 (d, J = 7.5 Hz, 1 H), 6.96 (d, J = 7.5 Hz, 1 H), 5.38 (d, J = 13.2 Hz, 1 H), 5.30 (d, J = 13.2 Hz, 1 H), 5.00 (t, J = 2.5 Hz, 1 H), 4.73 (t, J = 2.2 Hz, 1 H), 4.07 (s, 1 H), 2.86 (dd, J = 12.4, 4.8 Hz, 1 H), 2.33–2.23 (m, 1 H), 2.18 (dd, J = 10.2, 2.2 Hz, 1 H), 2.14 (d, J = 2.0 Hz, 1 H), 2.11 (s, 3 H), 2.05 (d, J = 11.8 Hz, 1 H), 1.98 (d, J = 5.2 Hz, 1 H), 1.95–1.92 (m, 1 H), 1.79–1.70 (m, 1 H), 1.65 (dd, J = 12.6, 5.2 Hz, 1 H), 1.57 (dd, J = 12.7, 5.2 Hz, 1 H). $^{13}\text{C-NMR}$ (100 MHz, CDCl_3): δ 171.1, 154.1, 147.9, 144.5, 143.0, 138.0, 135.0, 129.2, 129.0, 127.8, 124.0, 119.9, 103.5, 80.6, 77.6, 77.2, 76.8, 65.3, 54.7, 53.6, 52.3, 49.0, 39.5, 34.2, 22.1, 20.0. HRMS (ESI) m/z calcd for $\text{C}_{25}\text{H}_{26}\text{NO}_5$ $[\text{M} + \text{H}]^+$: 420.1811, found: 420.1815. m/z calcd for $\text{C}_{25}\text{H}_{25}\text{NO}_5\text{Na}$ $[\text{M} + \text{Na}]^+$: 442.1630, found: 442.1629.

4-Methylbenzyl(7*S*,9*a*S,10*R*)-7-hydroxy-1-methyl-8-methylene-4*b*,6,7,8,9,10-hexahydro-5*H*-7,9*a*-methanobenzo[*a*]azulene-10-carboxylate (**6c**). Yield: 75.7% as a colorless oily liquid. $^1\text{H-NMR}$ (400 MHz, CDCl_3): δ 7.35 (d, J = 8.0 Hz, 2 H), 7.22 (d, J = 7.9 Hz, 2 H), 7.18 (t, J = 7.5 Hz, 1 H), 7.05 (d, J = 7.5 Hz, 1 H), 6.97 (d, J = 7.3 Hz, 1 H), 5.27 (d, J = 12.1 Hz, 1 H), 5.21 (d, J = 12.0 Hz, 1 H), 5.05 (t, J = 2.7 Hz, 1 H), 4.77 (t, J = 2.2 Hz, 1 H), 4.03 (s, 1 H), 2.83 (dd, J = 12.4, 4.8 Hz, 1 H), 2.40 (s, 3 H), 2.30–2.21 (m, 3 H), 2.19 (s, 3 H), 2.10 (m, 1 H), 1.98 (d, J = 5.0 Hz, 1 H), 1.94 (d, J = 10.2 Hz, 1 H), 1.81–1.74 (m, 1 H), 1.63 (dd, J = 12.8, 5.1 Hz, 1 H), 1.50 (dd, J = 12.6, 5.0 Hz, 1 H). $^{13}\text{C-NMR}$ (100 MHz, CDCl_3): δ 171.2, 154.1, 144.5, 138.4, 138.2, 135.1, 132.8, 129.3, 129.0, 128.8, 127.5 (×2), 119.7 (×2), 103.4, 80.5, 66.7, 54.7, 53.5, 52.2, 48.8, 39.4, 34.1, 22.1, 21.3, 20.0. HRMS (ESI) m/z calcd for $\text{C}_{26}\text{H}_{28}\text{O}_3\text{Na}$ $[\text{M} + \text{Na}]^+$: 411.1931, found: 411.1931.

4-Bromobenzyl(7*S*,9*a*S,10*R*)-7-hydroxy-1-methyl-8-methylene-4*b*,6,7,8,9,10-hexahydro-5*H*-7,9*a*-methanobenzo[*a*]azulene-10-carboxylate (**6d**). Yield: 77.4% as a white solid. $^1\text{H-NMR}$ (400 MHz, CDCl_3): δ 7.52 (d, J = 8.4 Hz, 2 H), 7.30 (d, J = 8.6 Hz, 2 H), 7.15 (t, J = 7.5 Hz, 1 H), 7.02 (d, J = 7.6 Hz, 1 H), 6.95 (d, J = 7.3 Hz, 1 H), 5.20 (d, J = 5.3 Hz, 2 H), 5.00 (t, J = 2.5 Hz, 1 H), 4.74 (t, J = 2.5 Hz, 1 H), 4.02 (s, 1 H), 2.84 (dd, J = 12.5, 5.0 Hz, 1 H),

2.26 (dd, $J = 13.2, 1.8$ Hz, 1 H), 2.17–2.16 (m, 1 H), 2.14 (d, $J = 2.6$ Hz, 1 H), 2.12 (s, 3 H), 2.08 (d, $J = 4.2$ Hz, 1 H), 1.98 (dd, $J = 12.2, 5.1$ Hz, 1 H), 1.96–1.90 (m, 1 H), 1.77–1.71 (m, 1 H), 1.64 (dd, $J = 12.8, 5.0$ Hz, 1 H), 1.59 (d, $J = 5.2$ Hz, 1 H). $^{13}\text{C-NMR}$ (100 MHz, CDCl_3): δ 171.1, 154.2, 144.4, 138.1, 135.0, 134.7, 131.8 ($\times 2$), 130.4 ($\times 2$), 129.0, 127.5, 122.5, 119.7, 103.3, 80.5, 65.8, 54.6, 53.5, 52.1, 48.9, 39.3, 34.0, 22.0, 19.9. HRMS (ESI) m/z calcd for $\text{C}_{25}\text{H}_{25}\text{BrO}_3\text{Na}$ $[\text{M} + \text{Na}]^+$: 475.0879, 477.0862, found: 475.0868, 477.0853 (1:1).

4-Chlorobenzyl(7*S*,9*aS*,10*R*)-7-hydroxy-1-methyl-8-methylene-4*b*,6,7,8,9,10-hexahydro-5*H*-7,9*a*-methanobenzo[*a*]azulene-10-carboxylate (**6e**). Yield: 82.7% as a white solid. $^1\text{H-NMR}$ (400 MHz, CDCl_3): δ 7.36 (s, 4 H), 7.15 (t, $J = 7.5$ Hz, 1 H), 7.02 (d, $J = 7.5$ Hz, 1 H), 6.95 (d, $J = 7.3$ Hz, 1 H), 5.23 (d, $J = 12.3$ Hz, 1 H), 5.19 (d, $J = 12.3$ Hz, 1 H), 5.00 (t, $J = 2.5$ Hz, 1 H), 4.74 (t, $J = 2.0$ Hz, 1 H), 4.02 (s, 1 H), 2.84 (dd, $J = 12.6, 5.0$ Hz, 1 H), 2.25 (dd, $J = 13.2, 1.7$ Hz, 1 H), 2.16 (d, $J = 2.3$ Hz, 1 H), 2.14 (d, $J = 2.4$ Hz, 1 H), 2.12 (s, 3 H), 2.10–2.07 (m, 1 H), 1.98 (dd, $J = 12.2, 5.1$ Hz, 1 H), 1.93 (dd, $J = 9.4, 1.2$ Hz, 1 H), 1.77–1.70 (m, 1 H), 1.62 (d, $J = 4.9$ Hz, 1 H), 1.58 (dd, $J = 12.7, 5.2$ Hz, 1 H). $^{13}\text{C-NMR}$ (100 MHz, CDCl_3): δ 171.1, 154.2, 144.4, 138.1, 135.0, 134.4, 134.2, 130.1 ($\times 2$), 129.0, 128.8 ($\times 2$), 127.5, 119.7, 103.3, 80.5, 65.8, 54.6, 53.5, 52.2, 48.9, 39.3, 34.0, 22.0, 19.9. HRMS (ESI) m/z calcd for $\text{C}_{25}\text{H}_{25}\text{ClO}_3\text{Na}$ $[\text{M} + \text{Na}]^+$: 431.1384, 433.1366, found: 431.1385, 433.1369 (3:1).

3-(Trifluoromethyl)benzyl(7*S*,9*aS*,10*R*)-7-hydroxy-1-methyl-8-methylene-4*b*,6,7,8,9,10-hexahydro-5*H*-7,9*a*-methanobenzo[*a*]azulene-10-carboxylate (**6f**). Yield: 52.7% as a colorless oily liquid. $^1\text{H-NMR}$ (400 MHz, CDCl_3): δ 7.67 (s, 1 H), 7.59 (d, $J = 7.7$ Hz, 2 H), 7.52–7.47 (m, 1 H), 7.13 (t, $J = 7.5$ Hz, 1 H), 7.00 (d, $J = 7.4$ Hz, 1 H), 6.93 (d, $J = 7.3$ Hz, 1 H), 5.30 (d, $J = 12.6$ Hz, 1 H), 5.25 (d, $J = 12.5$ Hz, 1 H), 4.96 (t, $J = 2.6$ Hz, 1 H), 4.70 (t, $J = 2.0$ Hz, 1 H), 4.02 (s, 1 H), 2.83 (dd, $J = 12.4, 4.8$ Hz, 1 H), 2.23 (dd, $J = 13.2, 1.8$ Hz, 1 H), 2.13 (dd, $J = 9.8, 2.4$ Hz, 1 H), 2.10 (d, $J = 2.4$ Hz, 1 H), 2.09 (s, 3 H), 2.06–2.04 (m, 1 H), 1.97–1.93 (m, 1 H), 1.92 (d, $J = 2.8$ Hz, 1 H), 1.72 (ddd, $J = 9.9, 5.3, 2.6$ Hz, 1 H), 1.60 (d, $J = 6.2$ Hz, 1 H), 1.57 (d, $J = 5.2$ Hz, 1 H). $^{13}\text{C-NMR}$ (100 MHz, CDCl_3): δ 171.2, 154.2, 144.5, 138.2, 136.9, 135.1, 132.1, 129.3(2 C), 129.2 (2 C), 127.7(2 C), 125.4(q, $J = 260$ Hz, 1 C), 119.9, 103.4, 80.6, 65.8, 54.7, 53.6, 52.3, 49.1, 39.4, 34.2, 22.1, 20.0. HRMS (ESI) m/z calcd for $\text{C}_{26}\text{H}_{25}\text{F}_3\text{O}_3\text{Na}$ $[\text{M} + \text{Na}]^+$: 465.1648, found: 465.1645.

3-Methoxybenzyl(7*S*,9*aS*,10*R*)-7-hydroxy-1-methyl-8-methylene-4*b*,6,7,8,9,10-hexahydro-5*H*-7,9*a*-methanobenzo[*a*]azulene-10-carboxylate (**6g**). Yield: 58.2% as a yellow oily liquid. $^1\text{H-NMR}$ (400 MHz, CDCl_3): δ 7.34–7.26 (m, 2 H), 7.15 (t, $J = 7.6$ Hz, 1 H), 7.01 (t, $J = 8.7$ Hz, 2 H), 6.95 (d, $J = 7.5$ Hz, 1 H), 6.88 (dd, $J = 7.9, 2.1$ Hz, 1 H),

5.22 (d, $J = 4.0$ Hz, 2 H), 4.98 (t, $J = 2.5$ Hz, 1 H), 4.72 (t, $J = 2.0$ Hz, 1 H), 4.03 (s, 1 H), 3.82 (s, 3 H), 2.83 (dd, $J = 12.5, 5.0$ Hz, 1 H), 2.29–2.24 (m, 1 H), 2.22 (dd, $J = 5.0, 1.7$ Hz, 1 H), 2.18 (d, $J = 2.7$ Hz, 1 H), 2.15 (s, 3 H), 2.12 (d, $J = 2.6$ Hz, 1 H), 1.97 (dd, $J = 12.2, 5.1$ Hz, 1 H), 1.96–1.88 (m, 1 H), 1.73 (dd, $J = 11.8, 5.1$ Hz, 1 H), 1.63 (dd, $J = 12.8, 4.9$ Hz, 1 H), 1.57 (dd, $J = 12.7, 5.1$ Hz, 1 H). $^{13}\text{C-NMR}$ (100 MHz, CDCl_3): δ 171.2, 159.7, 154.3, 144.4, 138.2, 137.2, 135.1, 129.7, 129.0, 127.4, 120.9, 119.7, 114.1, 113.9, 103.2, 80.5, 66.5, 55.3, 54.6, 53.5, 52.1, 48.9, 39.2, 34.0, 22.0, 19.9. HRMS (ESI) m/z calcd for $\text{C}_{26}\text{H}_{28}\text{O}_4\text{Na}$ $[\text{M} + \text{Na}]^+$: 427.1880, found: 427.1881.

4-Cyanobenzyl(7*S*,9*aS*,10*R*)-7-hydroxy-1-methyl-8-methylene-4*b*,6,7,8,9,10-hexahydro-5*H*-7,9*a*-methanobenzo[*a*]azulene-10-carboxylate (**6h**). Yield: 58.1% as a white solid. $^1\text{H-NMR}$ (400 MHz, CDCl_3): δ 7.68 (d, $J = 8.3$ Hz, 2 H), 7.51 (d, $J = 8.3$ Hz, 2 H), 7.15 (t, $J = 7.6$ Hz, 1 H), 7.01 (d, $J = 7.5$ Hz, 1 H), 6.95 (d, $J = 7.3$ Hz, 1 H), 5.32 (d, $J = 13.1$ Hz, 1 H), 5.24 (d, $J = 13.1$ Hz, 1 H), 5.00 (t, $J = 2.5$ Hz, 1 H), 4.73 (t, $J = 1.9$ Hz, 1 H), 4.05 (s, 1 H), 2.85 (dd, $J = 12.4, 4.8$ Hz, 1 H), 2.28–2.22 (m, 1 H), 2.16 (dd, $J = 10.4, 2.3$ Hz, 1 H), 2.13 (d, $J = 2.3$ Hz, 1 H), 2.09 (s, 3 H), 2.07 (d, $J = 7.5$ Hz, 1 H), 1.98 (dd, $J = 12.4, 5.3$ Hz, 1 H), 1.95–1.90 (m, 1 H), 1.77–1.71 (m, 1 H), 1.62 (d, $J = 1.7$ Hz, 1 H), 1.57 (dd, $J = 12.7, 5.2$ Hz, 1 H). $^{13}\text{C-NMR}$ (100 MHz, CDCl_3): δ 171.2, 154.2, 144.6, 141.3, 138.2, 135.0, 132.6 ($\times 2$), 129.2, 129.0 ($\times 2$), 127.8, 120.0, 118.7, 112.1, 103.6, 80.5, 65.6, 54.7, 53.7, 52.3, 48.9, 39.8, 34.3, 22.2, 20.0. HRMS (ESI) m/z calcd for $\text{C}_{26}\text{H}_{25}\text{NO}_3\text{Na}$ $[\text{M} + \text{Na}]^+$: 422.1727, found: 422.1726.

2,3-Difluorobenzyl(7*S*,9*aS*,10*R*)-7-hydroxy-1-methyl-8-methylene-4*b*,6,7,8,9,10-hexahydro-5*H*-7,9*a*-methanobenzo[*a*]azulene-10-carboxylate (**6i**). Yield: 65.5% as a white solid. $^1\text{H-NMR}$ (400 MHz, CDCl_3): δ 7.27–7.22 (m, 1 H), 7.21–7.10 (m, 3 H), 7.05 (d, $J = 5.5$ Hz, 1 H), 6.98 (d, $J = 5.4$ Hz, 1 H), 5.39 (d, $J = 12.2$ Hz, 1 H), 5.31 (d, $J = 15.8$ Hz, 1 H), 5.04 (s, 1 H), 4.77 (s, 1 H), 4.06 (s, 1 H), 2.90–2.80 (m, 1 H), 2.37–2.22 (m, 3 H), 2.17 (s, 3 H), 2.10–2.05 (m, 1 H), 2.01 (dd, $J = 12.4, 5.5$ Hz, 1 H), 1.97 (d, $J = 4.9$ Hz, 1 H), 1.78 (d, $J = 11.2$ Hz, 1 H), 1.66 (d, $J = 4.0$ Hz, 1 H), 1.60 (d, $J = 12.4$ Hz, 1 H). $^{13}\text{C-NMR}$ (100 MHz, CDCl_3): δ 171.0, 154.3, 144.4, 138.1, 135.0, 129.0, 127.5, 125.8, 125.5, 125.3, 124.2(d, $J = 242$ Hz, 1 C), 119.7, 117.8, 117.6(d, $J = 238$ Hz, 1 C), 103.2, 80.5, 60.0, 54.6, 53.5, 52.2, 48.9, 39.3, 34.1, 22.0, 19.8. HRMS (ESI) m/z calcd for $\text{C}_{25}\text{H}_{24}\text{F}_2\text{O}_3\text{Na}$ $[\text{M} + \text{Na}]^+$: 433.1586, found: 433.1585.

3-Phenoxybenzyl(7*S*,9*aS*,10*R*)-7-hydroxy-1-methyl-8-methylene-4*b*,6,7,8,9,10-hexahydro-5*H*-7,9*a*-methanobenzo[*a*]azulene-10-carboxylate (**6j**). Yield: 41.5% as a yellow oily liquid. $^1\text{H-NMR}$ (400 MHz, CDCl_3): δ 7.42–7.34 (m, 3 H), 7.21–7.16 (m, 3 H), 7.14 (s, 1 H), 7.08 (d, $J = 8.5$ Hz, 3 H), 7.00 (dd, $J = 16.7, 8.5$ Hz, 2 H), 5.28 (d, $J = 12.4$ Hz,

1 H), 5.22 (d, $J = 12.4$ Hz, 1 H), 5.07 (s, 1 H), 4.79 (s, 1 H), 4.05 (s, 1 H), 2.82 (d, $J = 11.4$ Hz, 1 H), 2.31–2.22 (m, 3 H), 2.19 (s, 3 H), 2.08 (d, $J = 10.1$ Hz, 1 H), 2.04–1.98 (m, 1 H), 1.97–1.91 (m, 1 H), 1.79 (d, $J = 9.6$ Hz, 1 H), 1.70–1.58 (m, 1 H), 1.32 (t, $J = 7.1$ Hz, 1 H). $^{13}\text{C-NMR}$ (100 MHz, CDCl_3): δ 171.2, 157.6, 157.0, 154.3, 144.5, 138.3, 137.9, 135.0, 130.0, 130.0, 129.1, 127.5, 123.6, 123.2, 119.8, 119.1, 118.8, 118.7, 103.4, 80.5, 66.1, 54.7, 53.6, 52.2, 48.9, 39.5, 34.2, 22.1, 20.0.

General procedure for the preparation of substituted (3*S*,9*R*,9*aR*)-8-Methyl-2-methylene-11-oxo-1,2,3,9-tetrahydro-3,9*a*-ethanofluorene-9-carboxylate (**7a–7j**). The compounds **6a–6j** (1.20 mmol, 1 eq) and 2,3-dichloro-5,6-dicyanobenzoquinone (545 mg, 2.40 mmol, 2 eq) were dissolved in toluene (20 mL) in an oven-dried round bottom flask with a magnetic stirring bar (Cross and Markwell 1973). The reaction mixture was heated at 80 °C for 15 h. Then, the reaction was cooled to room temperature and was diluted with ethyl acetate (10 mL). The combined organic layer was washed with saturated aqueous ammonium chloride (2 × 20 mL) and water (4 × 10 mL), dried over anhydrous Na_2SO_4 and concentrated in a vacuum. The residue was purified by column chromatography (PE/EtOAc = 4:1–3:1) to afford derivatives **7a–7j**.

4-Benzyl (3*S*,9*R*,9*aR*)-8-methyl-2-methylene-11-oxo-1,2,3,9-tetrahydro-3,9*a*-ethanofluorene-9-carboxylate (7a). Yield: 78.0% as a yellow oily liquid. $[\alpha]_{\text{D}}^{25} = +73.5$ ($c = 1.0$, CH_3OH). $^1\text{H-NMR}$ (400 MHz, CDCl_3): δ 7.43–7.36 (m, 5 H), 7.33 (d, $J = 7.6$ Hz, 1 H), 7.26 (d, $J = 7.6$ Hz, 1 H), 7.15 (d, $J = 7.3$ Hz, 1 H), 6.35 (d, $J = 6.4$ Hz, 1 H), 5.27 (d, $J = 1.3$ Hz, 2 H), 5.10 (t, $J = 2.2$ Hz, 1 H), 4.84 (t, $J = 1.6$ Hz, 1 H), 4.11 (s, 1 H), 3.77 (d, $J = 6.4$ Hz, 1 H), 2.52 (d, $J = 17.8$ Hz, 1 H), 2.33 (d, $J = 2.2$ Hz, 2 H), 2.22–2.16 (m, 1 H), 2.15 (s, 3 H). $^{13}\text{C-NMR}$ (100 MHz, CDCl_3): δ 206.1, 171.3, 153.5, 142.4, 139.9, 136.4, 136.2, 135.6, 130.9, 129.1, 129.0(4) (×2), 128.9(8), 128.7 (×2), 119.1, 112.5, 111.3, 67.1, 60.3, 55.5, 48.9, 45.7, 35.3, 18.9. FTIR (MeOH): $\nu_{\text{max}} = 3428, 2923, 1725, 1648, 1454, 1376, 1315, 1255, 1232, 1188, 1147, 970, 891, 774, 751, 698, 657, 597$ cm^{-1} . HRMS (ESI) m/z calcd for $\text{C}_{25}\text{H}_{23}\text{O}_3$ [$\text{M} + \text{H}$] $^+$: 371.1642, found: 371.1662.

4-Nitrobenzyl(3*S*,9*R*,9*aR*)-8-methyl-2-methylene-11-oxo-1,2,3,9-tetrahydro-3,9*a*-ethanofluorene-9-carboxylate (7b). Yield: 97.5% as a white solid. $[\alpha]_{\text{D}}^{25} = +114.6$ ($c = 1.0$, CH_3OH). $^1\text{H-NMR}$ (400 MHz, CDCl_3): δ 8.23 (d, $J = 8.7$ Hz, 2 H), 7.53 (d, $J = 8.8$ Hz, 2 H), 7.33 (d, $J = 7.7$ Hz, 1 H), 7.27 (t, $J = 7.5$ Hz, 1 H), 7.13 (d, $J = 7.3$ Hz, 1 H), 6.35 (d, $J = 6.4$ Hz, 1 H), 5.37–5.28 (m, 2 H), 5.11 (t, $J = 2.5$ Hz, 1 H), 4.86 (t, $J = 2.5$ Hz, 1 H), 4.14 (s, 1 H), 3.78 (d, $J = 6.4$ Hz, 1 H), 2.51 (d, $J = 17.8$ Hz, 1 H), 2.41 (d, $J = 15.7$ Hz, 1 H), 2.34 (dd, $J = 15.9, 2.4$ Hz, 1 H), 2.22 (dd, $J = 17.8, 2.9$ Hz, 1 H), 2.11 (s, 3 H). $^{13}\text{C-NMR}$ (100 MHz, CDCl_3): δ 205.7, 171.1, 153.3, 148.1, 142.7, 142.1, 139.7,

136.5, 136.0, 131.1, 129.3(3), 129.3 (×2), 124.0 (×2), 119.4, 112.9, 111.7, 65.5, 60.3, 55.5, 48.9, 45.7, 35.5, 19.0. FTIR (MeOH): $\nu_{\text{max}} = 3361, 2921, 2851, 2360, 1729, 1649, 1521, 1457, 1347, 1318, 1257, 1230, 1188, 1149, 1027, 894, 847, 776, 738, 699, 657$ cm^{-1} . HRMS (ESI) m/z calcd for $\text{C}_{25}\text{H}_{22}\text{NO}_5$ [$\text{M} + \text{H}$] $^+$: 416.1498, found: 416.1498. m/z calcd for $\text{C}_{25}\text{H}_{21}\text{NO}_5\text{Na}$ [$\text{M} + \text{Na}$] $^+$: 438.1317, found: 438.1315.

4-Methylbenzyl(3*S*,9*R*,9*aR*)-8-methyl-2-methylene-11-oxo-1,2,3,9-tetrahydro-3,9*a*-ethanofluorene-9-carboxylate (7c). Yield: 85.8% as a yellow oily liquid. $[\alpha]_{\text{D}}^{25} = +176.8$ ($c = 2.0$, CH_3OH). $^1\text{H-NMR}$ (400 MHz, CDCl_3): δ 7.33 (d, $J = 4.3$ Hz, 1 H), 7.31 (d, $J = 3.5$ Hz, 2 H), 7.25 (t, $J = 7.5$ Hz, 1 H), 7.20 (d, $J = 7.9$ Hz, 2 H), 7.14 (d, $J = 7.3$ Hz, 1 H), 6.32 (d, $J = 6.4$ Hz, 1 H), 5.31–5.19 (m, 1 H), 5.12 (t, $J = 2.5$ Hz, 1 H), 4.85 (t, $J = 2.5$ Hz, 1 H), 4.12 (s, 1 H), 3.79 (d, $J = 6.4$ Hz, 1 H), 2.49 (d, $J = 17.8$ Hz, 1 H), 2.39 (s, 3 H), 2.34 (s, 2 H), 2.19 (s, 3 H), 2.14 (d, $J = 3.1$ Hz, 1 H). $^{13}\text{C-NMR}$ (100 MHz, CDCl_3): δ 205.9, 171.2, 153.4, 142.5, 140.1, 138.4, 136.3, 136.1, 132.6, 132.6, 130.8, 129.3(2) (×2), 129.2(8), 128.9, 119.1, 112.4, 111.1, 66.8, 60.2, 55.3, 48.8, 45.4, 35.2, 21.3, 18.9. FTIR (MeOH): $\nu_{\text{max}} = 3419, 2920, 1725, 1648, 1517, 1451, 1375, 1316, 1232, 1188, 1147, 1068, 970, 889, 845, 804, 774, 657, 547$ cm^{-1} . HRMS (ESI) m/z calcd for $\text{C}_{26}\text{H}_{25}\text{O}_3$ [$\text{M} + \text{H}$] $^+$: 385.1798, found: 385.1798.

4-Bromobenzyl(3*S*,9*R*,9*aR*)-8-methyl-2-methylene-11-oxo-1,2,3,9-tetrahydro-3,9*a*-ethanofluorene-9-carboxylate (7d). Yield: 77.7% as a colorless crystalline solid. $[\alpha]_{\text{D}}^{25} = +160.2$ ($c = 2.0$, CH_3OH). $^1\text{H-NMR}$ (400 MHz, CDCl_3): δ 7.52 (d, $J = 8.4$ Hz, 2 H), 7.33 (d, $J = 7.5$ Hz, 1 H), 7.29 (d, $J = 7.2$ Hz, 1 H), 7.27 (m, 2 H), 7.14 (d, $J = 7.3$ Hz, 1 H), 6.35 (d, $J = 6.4$ Hz, 1 H), 5.20 (m, 2 H), 5.11 (t, $J = 2.3$ Hz, 1 H), 4.85 (t, $J = 1.8$ Hz, 1 H), 4.09 (s, 1 H), 3.78 (d, $J = 6.4$ Hz, 1 H), 2.50 (d, $J = 17.7$ Hz, 1 H), 2.31–2.28 (m, 2 H), 2.21 (dd, $J = 17.6, 2.3$ Hz, 1 H), 2.13 (s, 3 H). $^{13}\text{C-NMR}$ (100 MHz, CDCl_3): δ 205.7, 171.1, 153.2, 142.1, 139.7, 136.3, 136.0, 134.4, 131.8 (×2), 130.8, 130.7 (×2), 129.0, 122.8, 119.0, 112.5, 111.3, 66.1, 60.1, 55.3, 48.7, 45.5, 35.2, 18.8. FTIR (MeOH): $\nu_{\text{max}} = 3363, 2920, 1725, 1648, 1592, 1487, 1454, 1373, 1316, 1230, 1188, 1145, 1070, 974, 890, 842, 801, 774, 657, 548$ cm^{-1} . HRMS (ESI) m/z calcd for $\text{C}_{25}\text{H}_{21}\text{BrO}_3\text{Na}$ [$\text{M} + \text{Na}$] $^+$: 471.0566, 473.0549, found: 471.0565, 473.0552 (1:1).

4-Chlorobenzyl(3*S*,9*R*,9*aR*)-8-methyl-2-methylene-11-oxo-1,2,3,9-tetrahydro-3,9*a*-ethanofluorene-9-carboxylate (7e). Yield: 68.3% as a colorless crystalline solid. $[\alpha]_{\text{D}}^{25} = +180.5$ ($c = 1.0$, CH_3OH). $^1\text{H-NMR}$ (400 MHz, CDCl_3): δ 7.37 (d, $J = 8.8$ Hz, 2 H), 7.35–7.31 (m, 3 H), 7.26 (d, $J = 7.6$ Hz, 1 H), 7.14 (d, $J = 7.3$ Hz, 1 H), 6.35 (d, $J = 6.4$ Hz, 1 H), 5.22 (m, 2 H), 5.11 (t, $J = 2.3$ Hz, 1 H), 4.85 (t, $J = 1.7$ Hz, 1 H), 4.09 (s, 1 H), 3.78 (d, $J = 6.4$ Hz, 1 H), 2.50 (d, $J = 17.7$ Hz, 1 H), 2.30 (m, 2 H), 2.21 (dd, $J = 17.8,$

1.0 Hz, 1 H), 2.13 (s, 3 H). $^{13}\text{C-NMR}$ (100 MHz, CDCl_3): δ 205.7, 171.1, 153.2, 142.1, 139.7, 136.3, 136.0, 134.6, 133.9, 130.8, 130.4 ($\times 2$), 129.0, 128.8 ($\times 2$), 119.0, 112.5, 111.3, 66.0, 60.1, 55.4, 48.7, 45.5, 35.2, 18.8. FTIR (MeOH): ν_{max} = 3425, 2910, 1728, 1648, 1493, 1456, 1406, 1374, 1317, 1254, 1188, 1148, 1090, 974, 891, 844, 805, 774, 657, 535 cm^{-1} . HRMS (ESI) m/z calcd for $\text{C}_{25}\text{H}_{21}\text{ClO}_3\text{Na}$ $[\text{M} + \text{Na}]^+$: 427.1071, 429.1053, found: 427.1077, 429.1056 (3:1).

3-(Trifluoromethyl)benzyl(3S,9R,9aR)-8-methyl-2-methylene-11-oxo-1,2,3,9-tetrahydro-3,9a-ethanofluorene-9-carboxylate (7f). Yield: 64.4% as a colorless oily liquid. $[\alpha]_{\text{D}}^{25} = +138.3$ ($c = 2.0$, CH_3OH). $^1\text{H-NMR}$ (400 MHz, CDCl_3): δ 7.64 (d, $J = 7.0$ Hz, 2 H), 7.59 (d, $J = 7.6$ Hz, 1 H), 7.55–7.49 (m, 1 H), 7.33 (d, $J = 7.6$ Hz, 1 H), 7.28 (t, $J = 7.5$ Hz, 1 H), 7.15 (d, $J = 7.2$ Hz, 1 H), 6.36 (d, $J = 6.4$ Hz, 1 H), 5.34–5.27 (m, 2 H), 5.11 (t, $J = 2.5$ Hz, 1 H), 4.86 (t, $J = 2.5$ Hz, 1 H), 4.13 (s, 1 H), 3.78 (d, $J = 6.4$ Hz, 1 H), 2.51 (d, $J = 17.8$ Hz, 1 H), 2.38–2.27 (m, 2 H), 2.18 (d, $J = 12.2$ Hz, 1 H), 2.12 (s, 3 H). $^{13}\text{C-NMR}$ (100 MHz, CDCl_3): δ 206.6, 171.1, 153.3, 142.1, 139.7, 136.6, 136.4, 136.0, 132.1, 132.1, 130.9 (2 C), 129.3, 129.1, 125.5 (q, $J = 267$ Hz, 1 C), 120.5, 119.2, 112.6, 111.4, 66.0, 60.2, 55.5, 48.8, 45.6, 35.4, 18.8. FTIR (MeOH): ν_{max} = 3440, 2926, 1730, 1649, 1453, 1377, 1330, 1257, 1202, 1160, 1125, 1100, 1073, 1027, 980, 891, 800, 776, 702, 659, 548 cm^{-1} . HRMS (ESI) m/z calcd for $\text{C}_{26}\text{H}_{22}\text{F}_3\text{O}_3$ $[\text{M} + \text{H}]^+$: 439.1516, found: 439.1515.

3-Methoxybenzyl(3S,9R,9aR)-8-methyl-2-methylene-11-oxo-1,2,3,9-tetrahydro-3,9a-ethanofluorene-9-carboxylate (7g). Yield: 81.4% as a yellow oily liquid. $[\alpha]_{\text{D}}^{25} = +92.6$ ($c = 1.0$, CH_3OH). $^1\text{H-NMR}$ (400 MHz, CDCl_3): δ 7.33 (d, $J = 7.5$ Hz, 1 H), 7.26 (t, $J = 7.6$ Hz, 2 H), 7.14 (d, $J = 7.3$ Hz, 1 H), 6.99 (d, $J = 7.5$ Hz, 1 H), 6.96–6.88 (m, 2 H), 6.35 (d, $J = 6.4$ Hz, 1 H), 5.29–5.20 (m, 2 H), 5.11 (t, $J = 2.5$ Hz, 1 H), 4.87 (t, $J = 2.5$ Hz, 1 H), 4.13 (s, 1 H), 3.80 (s, 3 H), 3.78 (d, $J = 6.4$ Hz, 1 H), 2.52 (d, $J = 17.8$ Hz, 1 H), 2.40–2.35 (m, 2 H), 2.22 (dd, $J = 8.1$, 4.5 Hz, 1 H), 2.18 (s, 3 H). $^{13}\text{C-NMR}$ (100 MHz, CDCl_3): δ 205.8, 171.1, 159.8, 153.3, 142.3, 139.9, 137.0, 136.3, 136.0, 130.8, 129.7, 128.9, 121.0, 119.1, 114.2, 114.2, 112.4, 111.2, 66.8, 60.2, 55.4, 55.3, 48.8, 45.5, 35.3, 18.9. FTIR (MeOH): ν_{max} = 3358, 1728, 1648, 1602, 1490, 1458, 1375, 1318, 1268, 1190, 1152, 1042, 975, 776, 693 cm^{-1} . HRMS (ESI) m/z calcd for $\text{C}_{26}\text{H}_{25}\text{O}_4$ $[\text{M} + \text{H}]^+$: 401.1747, found: 401.1745.

4-Cyanobenzyl(3S,9R,9aR)-8-methyl-2-methylene-11-oxo-1,2,3,9-tetrahydro-3,9a-ethanofluorene-9-carboxylate (7h). Yield: 80.3% as a yellow oily liquid. $[\alpha]_{\text{D}}^{25} = +175.5$ ($c = 1.0$, CH_3OH). $^1\text{H-NMR}$ (400 MHz, CDCl_3): δ 7.68 (d, $J = 8.1$ Hz, 2 H), 7.48 (d, $J = 8.1$ Hz, 2 H), 7.33 (d, $J = 7.6$ Hz, 1 H), 7.27 (t, $J = 7.5$ Hz, 1 H), 7.14 (d, $J = 7.2$ Hz, 1 H), 6.36 (d, $J = 6.4$ Hz, 1 H), 5.32–5.25 (m, 2 H), 5.12 (t, $J = 2.5$ Hz, 1 H), 4.86 (t, $J = 2.5$ Hz, 1 H), 4.12 (s, 1 H), 3.78

(d, $J = 6.4$ Hz, 1 H), 2.51 (d, $J = 17.8$ Hz, 1 H), 2.39–2.33 (m, 2 H), 2.22 (dd, $J = 17.8$, 2.6 Hz, 1 H), 2.10 (s, 3 H). $^{13}\text{C-NMR}$ (100 MHz, CDCl_3): δ 205.7, 171.1, 153.3, 142.1, 140.7, 139.7, 136.5, 136.0, 132.6 ($\times 2$), 131.0, 129.3 ($\times 2$), 129.2 ($\times 2$), 119.3, 112.8, 112.7, 111.6, 65.9, 60.3, 55.5, 48.9, 45.7, 35.5, 19.0. FTIR (MeOH): ν_{max} = 3349, 2228, 1726, 1644, 1455, 1376, 1319, 1257, 1188, 1147, 979, 818, 775, 548 cm^{-1} . HRMS (ESI) m/z calcd for $\text{C}_{26}\text{H}_{21}\text{NO}_3\text{Na}$ $[\text{M} + \text{H}]^+$: 418.1414, found: 418.1413.

2,3-Difluorobenzyl (3S,9R,9aR)-8-methyl-2-methylene-11-oxo-1,2,3,9-tetrahydro-3,9a-ethanofluorene-9-carboxylate (7i). Yield: 67.5% as a colorless oily liquid. $[\alpha]_{\text{D}}^{25} = +85.1$ ($c = 1.0$, CH_3OH). $^1\text{H-NMR}$ (400 MHz, CDCl_3): δ 7.40–7.23 (m, 2 H), 7.18 (d, $J = 3.5$ Hz, 2 H), 7.13 (d, $J = 7.0$ Hz, 2 H), 6.34 (d, $J = 6.3$ Hz, 1 H), 5.33 (d, $J = 3.1$ Hz, 2 H), 5.12 (t, $J = 2.5$ Hz, 1 H), 4.90 (t, $J = 2.5$ Hz, 1 H), 4.12 (s, 1 H), 3.78 (d, $J = 6.4$ Hz, 1 H), 2.51 (d, $J = 17.8$ Hz, 1 H), 2.46–2.28 (m, 2 H), 2.16 (s, 3 H), 1.90 (d, $J = 5.7$ Hz, 1 H). $^{13}\text{C-NMR}$ (100 MHz, CDCl_3): δ 205.8, 171.0, 153.2, 142.0, 139.7, 136.3, 136.0, 130.8, 129.0, 125.9, 125.1, 125.0, 124.3 (d, $J = 251$ Hz, 1 C), 119.0, 118.0, 117.8 (d, $J = 237$ Hz, 1 C), 112.5, 111.3, 60.2, 60.1, 55.2, 48.7, 45.4, 35.2, 18.7. FTIR (MeOH): ν_{max} = 3434, 2923, 1727, 1649, 1597, 1491, 1378, 1316, 1288, 1215, 1188, 1145, 1073, 1030, 977, 892, 828, 775, 731, 688, 657, 547 cm^{-1} . HRMS (ESI) m/z calcd for $\text{C}_{25}\text{H}_{20}\text{F}_2\text{O}_3\text{Na}$ $[\text{M} + \text{Na}]^+$: 429.1273, found: 429.1271.

3-Phenoxybenzyl (3S,9R,9aR)-8-methyl-2-methylene-11-oxo-1,2,3,9-tetrahydro-3,9a-ethanofluorene-9-carboxylate (7j). Yield: 59.5% as a yellow oily liquid. $[\alpha]_{\text{D}}^{25} = +100.2$ ($c = 1.0$, CH_3OH). $^1\text{H-NMR}$ (400 MHz, CDCl_3): δ 7.40–7.32 (m, 3 H), 7.15 (dd, $J = 14.6$, 7.3 Hz, 3 H), 7.02 (d, $J = 6.1$ Hz, 3 H), 6.35 (d, $J = 6.2$ Hz, 1 H), 5.23 (q, $J = 12.2$ Hz, 2 H), 5.12 (s, 1 H), 4.88 (s, 1 H), 4.10 (s, 1 H), 3.79 (d, $J = 6.4$ Hz, 1 H), 2.49 (d, $J = 17.9$ Hz, 1 H), 2.35 (s, 2 H), 2.21 (d, $J = 18.0$ Hz, 1 H), 2.14 (s, 3 H). $^{13}\text{C-NMR}$ (100 MHz, CDCl_3): δ 205.7, 171.0, 157.7, 156.8, 153.3, 142.2, 139.8, 137.4, 136.6, 136.3, 136.0, 130.8, 130.0, 129.9, 128.9, 123.7, 123.3, 121.0, 119.2, 119.0, 118.8, 118.7, 112.4, 111.2, 66.4, 60.2, 55.4, 48.7, 45.5, 35.3, 18.8. FTIR (MeOH): ν_{max} = 3368, 2922, 2852, 1728, 1648, 1584, 1486, 1447, 1375, 1315, 1256, 1214, 1188, 1146, 1070, 976, 936, 889, 774, 693, 657, 548 cm^{-1} . HRMS (ESI) m/z calcd for $\text{C}_{31}\text{H}_{26}\text{O}_4\text{Na}$ $[\text{M} + \text{Na}]^+$: 485.1723, found: 485.1725.

Crystallography studies

Single crystals of $\text{C}_{23}\text{H}_{31}\text{NO}_2$ [3c] and $\text{C}_{25}\text{H}_{21}\text{BrO}_3$ [7d] were prepared. A suitable crystal was selected and collected on an Oxford Diffraction SuperNova, Dual, AtlasS2 diffractometer using Cu at zero. The crystal was kept at 100.00 K using an Oxford Cryosystems cooling device during data collection.

Crystal Data for compound 3c: $C_{23}H_{31}NO_2$, $M = 353.49$, $T = 100.00(10)$ K, monoclinic, space group $P2_1$ (no. 4), $a = 9.41986(18)$ Å, $b = 10.71565(19)$ Å, $c = 20.4295(4)$ Å, $\beta = 91.3040(18)^\circ$, $V = 2061.62(7)$ Å³, $Z = 4$, $\mu(\text{CuK}\alpha) = 0.557$ mm⁻¹, $D_{\text{calc}} = 1.139$ g/cm³, 14090 reflections measured ($4.326^\circ \leq 2\theta \leq 146.806^\circ$), 7380 unique data ($R_{\text{int}} = 0.0271$, $R_{\text{sigma}} = 0.0336$) were used in all calculations. The final R_1 was 0.0552 [$I > 2\sigma(I)$] and wR_2 was 0.1477 (all data).

Crystal Data for compound 7d: $C_{25}H_{21}BrO_3$, $M = 449.33$, $T = 100.01(10)$ K, orthorhombic, space group $P2_12_12_1$ (no. 19), $a = 10.48757(15)$ Å, $b = 12.43058(18)$ Å, $c = 15.7993(2)$ Å, $V = 2059.70(5)$ Å³, $Z = 4$, $\mu(\text{CuK}\alpha) = 2.908$ mm⁻¹, $D_{\text{calc}} = 1.449$ g/cm³, 9762 reflections measured ($9.052^\circ \leq 2\theta \leq 147.118^\circ$), 4058 unique data ($R_{\text{int}} = 0.0200$, $R_{\text{sigma}} = 0.0229$) were used in all calculations. The final R_1 was 0.0254 [$I > 2\sigma(I)$] and wR_2 was 0.0653 (all data).

Biological assay

Cells and treatment protocol

HL-60 human promyelocytic leukemia cell line, SW480 human colon cancer cell line, and MCF-7 human breast cancer cell line were purchased from the cell bank of Sun Yat-sen University, China. NCI-H226 human lung cancer cell line was derived from the cell bank of Tsinghua University, China. They were cultured in RPMI-1640 containing FBS (10%) and penicillin/streptomycin (100 µg/mL) in a 5% CO₂ humidified atmosphere at 37 °C. DMSO was used as the vehicle to deliver the compounds at a final concentration of 0.1% in all experiments.

Measurement of antitumor activity against human tumor cell lines (MTT assay)

MTT assay was used to test the cytotoxicity of compounds on four human tumor cell lines (HL-60, NCI-H226, MCF-7, and SW480) (Kim et al. 2001; Cao et al. 2004). Cells were scattered in 96-well plates and then incubated in 10% medium (RPMI-1640) with various concentrations of the GA₃ derivative for 24 h. The viability of tumor cells dealt with MTT was measured by microplate spectrophotometer. The GA₃ derivatives synthesized in this study were tested at 1, 5, 10, 50, and 200 µM, and each test was repeated in triplicate.

Measurement of inhibitory activity against four RPTKs

Compounds **3d**, **3e**, **3f**, **7e**, **7f**, and **7g** were evaluated against four RPTKs including FGFR₁, ErbB₂, ALK, and KDR enzymes using FGFR₁, ErbB₂, ALK, and KDR Kit

(ELISA) according to the manufacturer's instructions (Kassab and Hassan 2018). All reagents, working standards and samples were prepared at first. First, 50 µL of each sample or standard was added to appropriate wells, and 100 µL of the antibody cocktail was added to each well. After the plate was sealed, it was incubated for 60 min at 37 °C on a plate shaker set to 400 rpm. Each well was washed with 3 × 350 µL buffer by aspirating or decanting from wells, then 300 µL wash buffer was dispensed into each well. Followed with this, 100 µL of 3,3',5,5'-tetramethylbenzidine substrate was added to each well, and the well was incubated for 10 min in the dark on a plate shaker which was set to 400 rpm at 4 °C. After 50 µL of stop solution was added, each plate was shaken on a plate shaker for 1 min to mix well. The OD value was recorded at 450 nm for 15 min and subtract average zero standard from all readings. These points was used to obtain a standard curve, which was used to calculate the protein concentrations of samples.

Data accessibility

The datasets supporting this article have been uploaded as part of the electronic supplementary material.

Acknowledgements We thank the Chinese National Natural Science Foundation (Grant 21801094), the Fundamental Research Funds for the Central Universities (China) (Grant 21617327) for generous financial support.

Compliance with ethical standards

Conflict of interest The authors declare that they have no conflict of interest.

Publisher's note Springer Nature remains neutral with regard to jurisdictional claims in published maps and institutional affiliations.

References

- Bon DJ-YD, Mander LN, Lan P (2018) Syntheses of gibberellins A₁₅ and A₂₄, the key metabolites in gibberellin biosynthesis. *J Org Chem* 83:6566–6572
- Cao R, Chen Q, Hou X, Chen H, Guan H, Ma Y, Peng W, Xu A (2004) Synthesis, acute toxicities, and antitumor effects of novel 9-substituted β-carboline derivatives. *Bioorg Med Chem* 12:4613–4623
- Chen H, Yang Z, Ding C, Chu L, Zhang Y, Terry K, Liu H, Shen Q, Zhou J (2013) Discovery of O-alkylamino tethered niclosamide derivatives as potent and orally bioavailable anticancer agents. *ACS Med Chem Lett* 4:180–185
- Chen J, Sun Z, Zhang Y, Zeng X, Qing C, Liu J, Li L, Zhang H (2009) Synthesis of gibberellin derivatives with anti-tumor bioactivities. *Bioorg Med Chem Lett* 19:5496–5499
- Cross BE, Grove JF, MacMillan J, Mulholland TPC (1958) Gibberellic acid. Part VII. Struct gibberic acid *J Chem Soc* 0:2520–2536
- Cross BE, Grove JF, Morrison A (1961) Gibberellic acid. Part XVIII. Some rearrangements of ring A. *J Chem Soc* 0:2498–2515

- Cross BE, Markwell RE (1973) Cheminform abstract: rearrangements of the gibbane skeleton during reactions with 2,3-dichloro-5,6-dicyanobenzoquinone (DDQ). *J Chem Soc, Perkin Trans 1* 0:1476–1487
- Egbewande FA, Sadowski MC, Levrier C, Tousignant KD, White JM, Coster MJ, Nelson CC, Davis RA (2018) Identification of gibberellic acid derivatives that deregulate cholesterol metabolism in prostate cancer cells. *J Nat Prod* 81:838–845
- Grigor'eva NY, Kucherov VF (1966) Gibberellins. *Russ Chem Rev* 35:850
- Gu ZM, Wu YL, Zhou MY, Liu CX, Xu HZ, Yan H, Zhao Y, Huang Y, Sun HD, Chen GQ (2010) Pharicin B stabilizes retinoic acid receptor- α and presents synergistic differentiation induction with ATRA in myeloid leukemic cells. *Blood* 116:5289–5297
- He F, Xiao W-L, Pu J-X, Wu Y-L, Zhang H-B, Li X-N, Zhao Y, Yang L-B, Chen G-Q, Sun H-D (2009) Cytotoxic ent-kaurane diterpenoids from *Isodon sinuolata*. *PYTCAS* 70:1462–1466
- Huigens Iii RW, Morrison KC, Hicklin RW, Flood Jr TA, Richter MF, Hergenrother PJ (2013) A ring-distortion strategy to construct stereochemically complex and structurally diverse compounds from natural products. *Nat Chem* 5:195–202
- Kassab AE, Hassan RA (2018) Novel benzotriazole N-acylarylhyazone hybrids: design, synthesis, anticancer activity, effects on cell cycle profile, caspase-3 mediated apoptosis and FAK inhibition. *Bioorg Chem* 80:531–544
- Kim D-K, Ryu DH, Lee JY, Lee N, Kim Y-W, Kim J-S, Chang K, Im G-J, Kim T-K, Choi W-S (2001) Synthesis and biological evaluation of novel A-ring modified hexacyclic camptothecin analogues. *J Med Chem* 44:1594–1602
- Krow GR (2004) The Baeyer–Villiger oxidation of ketones and aldehydes. *Org React* 43:251–798
- Lin Z-M, Guo Y-X, Gao Y-H et al. (2015) *ent*-kaurane diterpenoids from Chinese liverworts and their antitumor activities through Michael addition as detected in situ by a fluorescence probe. *J Med Chem* 58:3944–3956
- Liu M, Wang W-G, Sun H-D, Pu J-X (2017) Diterpenoids from isodon species: an update. *Nat Prod Rep.* 34:1090–1140
- Mandal PK, Ren Z, Chen X, Xiong C, McMurry JS (2009) Structure-affinity relationships of glutamine mimics incorporated into phosphopeptides targeted to the sh2 domain of signal transducer and activator of transcription 3. *J Med Chem* 52:6126–6141
- Mander LN (1992) The chemistry of gibberellins: an overview. *Chem Rev* 92:573–612
- Mander LN (2003) Twenty years of gibberellin research. *Nat Prod Rep.* 20:49–69
- Mo F, Dong G (2014) ChemInform abstract: regioselective ketone α -alkylation with simple olefins via dual activation. *Science* 345:68–72
- Mulholland TPC (1958) Gibberellic acid. Part II. *Struct Synth Gibberene J Chem Soc* 0:2693–2701
- Sun H, Zhou Q, Fujita T, Takeda Y, Minami Y, Maronaka T, Lin Z, Shen X (1992) Rubescensin d, a diterpenoid from *rabdosia rubescens*. *PYTCAS* 31:1418–1419
- Wu M-J, Wu D-M, Chen J-B, Zhao J-F, Gong L, Gong Y-X, Li Y, Yang X-D, Zhang H (2018) Synthesis and anti-proliferative activity of allogibberic acid derivatives containing 1,2,3-triazole pharmacophore. *Bioorg Med Chem Lett* 28:2543–2549
- Wu Z, Zhang Y, Yang L et al. (2017) Three new *ent*-kaurane diterpenes from the herbs of *Wedelia prostrata*. *J Nat Med* 71:305–309
- Xie L, Chen Y, Chen J, Zhang H, Liao Y, Zhou Y, Zhou L, Qing C (2018) Anti-tumor effects and mechanism of GA-13315, a novel gibberellin derivative, in human lung adenocarcinoma: an in vitro and in vivo study. *Cell Mol Biol Lett* 24:6